Sommario

La struttura dei cromosomi e l'espressione genica sono influenzati dall'attività del rimodellatore della cromatina ATP-dipentente ISWI, altamente conservato negli eucarioti[1].
Negli eucarioti superiori ISWI è una proteina ubiquitaria, abbondante e necessaria per la vitalità cellulare [2, 3]. *In vitro*, ISWI usa l'energia proveniente dall'idrolisi dell'ATP per catalizzare reazioni di "spacing" and "sliding" dei nucleosomi [4].
In *Drosophila melanogaster* la mancanza della proteina ISWI è in grado di determinare *in vivo* una profonda alterazione dei livelli trascrizionali di alcuni geni ed una drammatica perdita della struttura complessiva dei cromosomi, facendoli così apparire altamente decondensati, in particolar modo il cromosoma X dei maschi (Figura 1) [2]. Tali difetti sono probabilmente imputabili all'attività di *"spacing"* nucleosomale di ISWI.
Nonostante i dati presenti in letteratura, ad oggi non è ancora chiaro come sia l'attività di regolatore trascrizionale che di determinante della struttura cromatinica di ISWI siano associabili con il suo legame alla cromatina e la sua capacità di spaziare i nucleosomi.

Pertanto, al fine di chiarire se i difetti della condensazione dei cromosomi e l'alterazione dell'espressione genica indotti dall'assenza di ISWI siano direttamente correlati con la sua attività di spaziatore dei nucleosomi, è stata condotta su scala genomica l'identificazione dei siti di legame della proteina ISWI alla cromatina (ChIP-chip) utilizzando come organismo modello la *Drosophila melanogaster*. Inoltre è stata condotta anche l'analisi dei cambiamenti nel posizionamento dei nucleosomi indotti dalla mutazione *ISWI*

L’analisi ChIP-chip su scala genomica ha rilevato circa 1.200 siti cromatinici altamente legati da ISWI, comprendenti regioni geniche ed intergeniche. Inoltre, sono state identificate diverse sequenze di DNA consenso legate in maniera preferenziale da ISWI.

I risultati ottenuti in questo studio dimostrano che ISWI lega i geni target preferenzialmente vicino al loro promotore causando delle locali alterazioni del posizionamento dei nucleosomi a livello del sito di inizio della trascrizione (TSS), fornendo così una possibile spiegazione molecolare della regolazione dell’espressione genica da parte di ISWI. Inoltre, dai dati si evince che le maggiori differenze del posizionamento nucleosomale indotte dalla mutazione *ISWI* sono a carico del cromosoma X, per tutti i geni analizzati legati da ISWI. In particolare, tra questi geni vi sono quelli regolati dal complesso di compensazione del dosaggio. Pertanto i risultati da me ottenuti sono compatibili con un modello secondo il quale l’attività di ISWI è necessaria al mantenimento del TSS di questi geni in uno stato privo di nucleosomi. La maggiore attività di ISWI sui geni della compensazione del dosaggio potrebbero altresì spiegare la particolare sensibilità del cromosoma X dei maschi alla perdita di ISWI.

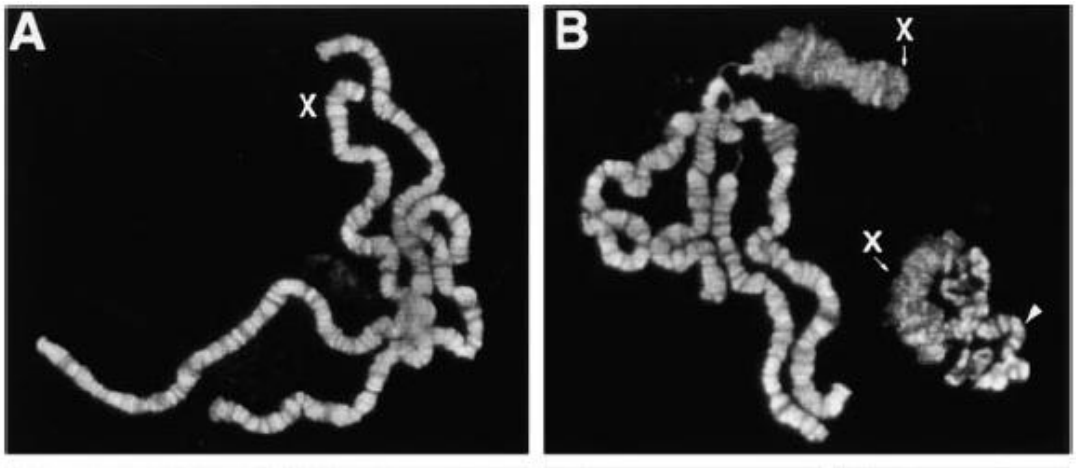

Figura 1: Effetti dell’assenza di ISWI sulla struttura dei cromosomi. Cromosomi politenici femminili **(A)** e maschili **(B)** di *Drosophila* preparati da ghiandole salivari di larve al

terzo stadio di sviluppo mutati in *ISWI*. Le frecce indicano la struttura cromosomica altamente decondensata ed alterata del cromosoma X dei maschi di larve mutate in *ISWI*. *Figura adattata da* [5].

Introduction

The eukariotic chromatin

In eukaryotic cells, DNA is packaged into highly compacted and condensed nucleoprotein structure called chromatin [6]. The basic repeating unit of chromatin is the nucleosome, which consists of about 150 bp of DNA wrapped around a core of histone octamer composed of two copies of each histone (H2A, H2B, H3 and H4). Nucleosomes are linked by 20–100 base pairs (bp) of linker DNA, forming a nucleosomal array (Figure 2) [7].

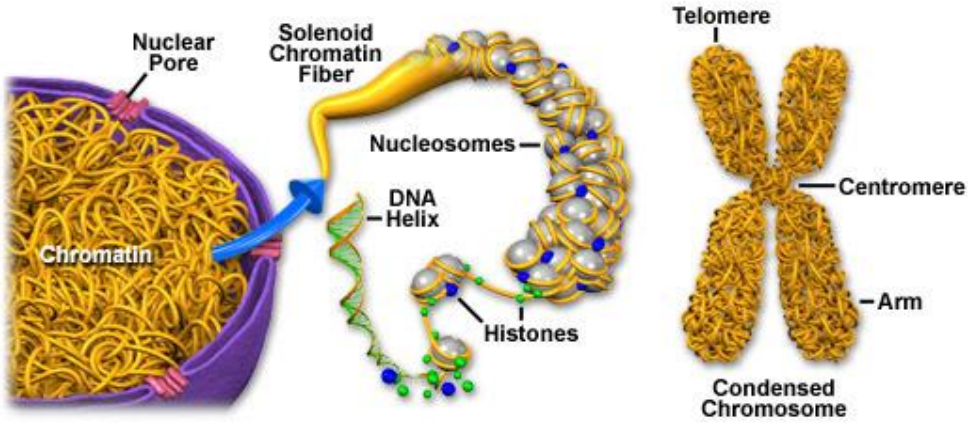

Figure 2: Chromatin and condensed chromosome structure. Each DNA strand wraps around groups of small protein molecules called "histones", forming a series of bead-like structures, called "nucleosomes", connected by the DNA strand. Consequently, during interphase, DNA is combined with proteins and organized into a precise, compact structure, a dense string-like fiber called "chromatin", which condenses even further into "chromosomes" during cell division.

The packaging of DNA into nucleosomes and higher-order chromatin structures allows the cell to organize its large and complex genome in the nucleus, but it represents also a barrier to DNA accesibility for all nuclear processes such as DNA replication, repair, recombination, and RNA transcription [7]. Therefore, eucaryotes have evolved regulatory mechanisms able to induce structural changes to chromatin in response to

environmental and cellular stimuli. Two distinct main activities are responsable of chromatin dynamics (Figure 3) [8, 9]. The first group of remodelers covalently modify by acetylation, phosphorylation, ubiquitination, ADP-ribosylation, and methylation the histone N-terminal [9]. The second group of remodelers uses the hydrolysis of ATP to induce movement of histone octamers relative to DNA in order to make the DNA accessible [10]. The enzymes that modulate chromatin accessibility using the energy of ATP hydrolysis are multiprotein complexes named ATP-dependent chromatin remodelers [11].

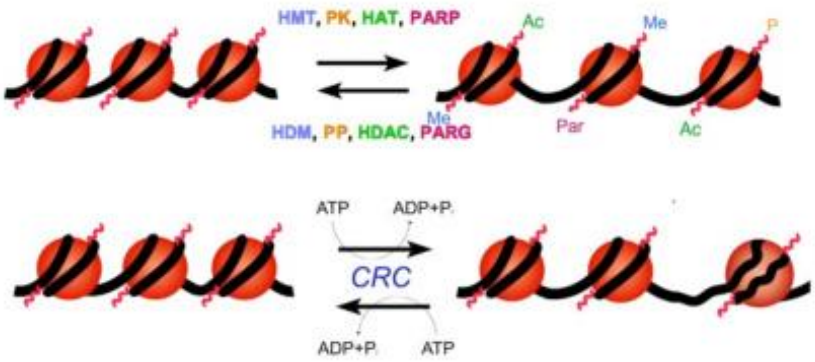

Figure 3: The two distinct mechanisms of chromatin remodeling. The two classes of highly conserved nucleosome remodeling enzyme that modulate chromatin accessibility and dynamics.

Even if these mechanisms are distinct, they are functionally interconnected inside the cell. These two functions can co-exist in the same multiproteic complex or reside in separate complexes, aniway they are both required to regulate chromatin structure and to mediate the activation of transcription, DNA replication and repair. These chromatin modifications, which occur without changes in DNA sequence, set different chromatin functional states and constitute the epigenetic marks of our genome [12, 13].

Chromatin and transcription

Proper gene expression is essential for normal growth and development. Chromatin packaging plays a central role in transcriptional regulation [14].

The nucleosome is one of the most stable protein-DNA complex under physiological conditions, however, the chromatin is not a simple static structure. It possesses dynamic properties that are tightly regulated by multiple mechanisms including histone modification, ATP-dependent remodeling, but also histone variant incorporation, and histone eviction [15].

Both histone tails and globular domains are subject to a broad range of post-translational modifications that are associated with active transcription, such as acetylation of histone 3 and histone 4 (H3 and H4) or di-trimethylation (me) of H3K4, are commonly referred to as euchromatin modifications. Modifications that are localized to inactive genes or regions, such as H3 K9me and H3 K27me, are often termed heterochromatin modifications [16]. Indeed, a specific histone modification is tightly regulated and is crucial for its effect on transcription. An additional level of complexity of transcriptional regulation is that individual histone modifications or modification patterns might be read by other factors. For example, acetylation of H4 K16 impairs the efficiency of ATP-dependent chromatin assembly and mononucleosome mobilization by the ACF histone chaperone [17], suggesting as single modifications can elicit multiple effects on chromatin structure.

The protein complexes that utilize ATP hydrolysis to alter the histone-DNA contacts are the second major class of chromatin regulators, they are generally referred to as chromatin-remodeling complexes [18] (see Table

1).

The consequences of remodeling include transient unwrapping of the end DNA from histone octamers, forming the DNA loop, or moving nucleosomes to different translational positions (sliding), all of which change the accessibility of nucleosomal DNA to transcription factors (TFs).

	Yeast		Drosophila		Human	
	Complex	ATPase	Complex	ATPase	Complex	ATPase
SWI/SNF subfamily	*SWI/SNF*	*Swi2/Snf2*	dSWI/*SNF*	Brahma	hSWI/*SNF*-A (BAF)	hBRG1, hBRM
	RSC	Sth1			hSWI/*SNF*-B (PBAF)	hBRG1
					p400.com	p400
ISWI subfamily	yISW1	Isw1	NURF	ISWI	RSF	hSNF2H
	yISW2	Isw2	CHRAC	ISWI	hCHRAC	hSNF2H
			ACF	ISWI	hACF	hSNF2H
					hWCRF	hSNF2H
					NoRC	hSNF2H
CHD/Mi-2 subfamily	CHD1	Chd1	dMi-2	dMi-2	NURD (NuRD, NUD)	CHD3/4 (Mi-2α/β)
INO80 subfamily	Ino80.com	Ino80		dIno80		hINO80

Table 1: Summery of the ATP-dependent chromatin remodeling complexes. *Picture adapted from* [19].

Several *in vivo* experiments in *S. cerevisiae* established a role for SWI/SNF chromatin remodeling complexes in gene activation by altering chromatin structure [20]. In *yeast*, microarray gene expression analysis suggested that SWI/SNF is required for activation and repression of different subsets of genes [21]. In *humans*, SWI/SNF complexes copurify with histone deacetylases that are linked to gene repression [22]. Furthermore, SWI/SNF function is necessary for the repression of cell cycle genes by the retinoblastoma protein (Rb) [23]. Therefore, no individual factors are able to play dominant role in generating the high specificity required to regulate transcription in

eukaryotes. Distinct multiprotein complexes are needed to modulate higher-order chromatin structure, to promoters or enhancers binding, to recruit both activators and repressors of transcription start sites, to modify nucleosomal structure, and to generate transcripts. Each of these complexes is a key player in regulating a given gene. Then all these complexes can work together to ensure proper regulation.

Chromatin remodeling and cancer

Traditionally, cancer has been viewed as a genetic disease caused by the sequential acquisition of mutations, leading to the constitutive activation of oncogenes and the loss of function of tumor suppressor genes [24]. However, it has become clear that "epigenetic alterations" also play a key role in the oncogenic transformation [25]. These epigenetic changes refers to modifications in genome function that occur without changes in DNA [12]. Several chromatin-remodeling mechanisms are reviewed in relation to their association with cancer, namely, DNA methylation, histone acetylation, methylation, phosphorylation and ATP-dependent chromatin remodeling [26]. As these changes typically occur simultaneously at numerous genetic loci, it is challenging to understand the mechanism by which they directly contribute to oncogenesis. However, some clear relationships between different chromatin-remodeling mechanisms alterations and cancer are beginning to appear.

The clearest functional link between the chromatin remodeling complexes and cancer comes from Snf5 studies. Snf5 is the catalytic subunit of SWI/SNF complex which uses the energy of ATP to mobilize nucleosomes and regulate transcription. A link between SNF5 and oncogenesis first emerged through examination of human tumors [27]. Specific inactivating mutations in SNF5 were identified in the large majority of malignant rhabdoid tumors [28]. Other studies showed that BRG1, the catalytic subunit of the *human* SWI/SNF complex is silenced in 10–20% of lung cancer as well as in a subset of breast, prostate and pancreatic cancers [29]. Moreover, the SWI/SNF complex is associated with multiple cancer-related pathways. *In vitro* evidences indicate that SWI/SNF complexes directly interact with tumour suppressors and oncogenes, such as RB, BRCA1, c-MYC and MLL9 [29] . *hSnf5* is

considered a tumour-suppressor gene, whose mutation or deletion stimulates cell-cycle progression, cooperating with P53 loss in oncogenic transformation [30].

Relevant links are also observed between ISWI complexes and cancer. SNF2H, the catalytic subunit of the human ISWI complex might suppress the effects of *Rb* loss or the oncogene *ras* in human cells [31]. It was found a significant increase of ISWI homologous (SNF2L and SNF2H) proteins in prostatic intraepithelial neoplasia and prostate adenocarcinoma [32]. SNF2H is expressed in all tested immortal or tumour-derived cell lines and is up-regulated in CD34 hematopoietic progenitors of acute myeloid leukemia patients [33].

Increasing data support the idea that the alterations of ATP-dependent chromatin remodelers play a key role in the cancer development. Moreover chromatin remodeling complexes have also roles in different cellular functions. The *yeast* ATPase chromatin remodeling complex INO80 has been shown to participate in DNA repair following DNA damage and a mammalian homolog has recently been identified [34-36]. The ISWI chromatin remodeling complex functions in DNA transcription and the Mi 2/ CHD chromatin remodeling complex has been identified as a central component of the *C. elegans* NURD repressor complex [37]. Gaining insights on the various functions of chromatin remodeling complexes and improving understanding of the interplay between different types of epigenetic modifications could better elucidate the mechanisms underlying cellular differentiation and also provide insight into disease, such as cancer, onset.

Chromatin remodelig by ISWI complexes

The term “chromatin remodeling” generally refers to a change in histone–DNA interactions inside the nucleosome. To promote DNA-directed processes in chromatin, it is often necessary to rearrange or to mobilize tnucleosomes. The nucleosomes remodeling is achieved by the action of chromatin-remodeling complexes, which are a family of ATP-dependent molecular machines [38].

In the eukaryotic nucleus, diverse chromatin remodeling machineries exists to translocate, remove or assemble nucleosomes. In *Saccharomyces cerevisiae* there is a minimum of nine or more different ATP-dependent chromatin remodelers and in humans the lowest estimate is well over 30 different complexes [10]. The chromatin remoleling activity is centered around an ATP-driven molecular machines that can move the nucleosomal DNA with respect to the histone octamer core via an ATP-driven mechanism. Four different families of chromatin remodeling complexes are conserved from *yeast* to human (Table 1). All four utilize ATP hydrolysis to alter histone-DNA contacts and share a similar ATPase domain (Figure 4). Each family is specialized for particular purposes and biological context, imparted by unique domains residing in their catalytic ATPases and also by their unique associated subunits [39].

One of the best conserved ATPase families involved in chromatin remodeling is the Imitation Switch (ISWI) family [40].

The ISWI chromatin remodeling ATPase was first identified in *Drosophila* due to its sequence homology to the *yeast* SWI2/SNF2 enzyme [41].

ISWI remodelers exist in all eukaryotes [10]. In *Drosophila*, ISWI is a component of three known chromatin remodeling complexes: NURF

(NUcleosome Remodeling Factor), ACF (ATP-utilizing Chromatin assembly and remodeling Factor) and CHRAC (CHRomatin Accessibility Complex) [42-45] (Table 1). In these complexes ISWI serves as the ATP-dependent motor that drives nucleosome assembly or changes in nucleosome structure. ISWI cooperates with other complex subunits to confer the specific activities of NURF, ACF and CHRAC.

Drosophila ISWI contains a number of domains and sequence motifs that are conserved among the ISWI subfamily [10] (Figure 4).
All ISWI proteins contain a conserved ATPase domain that belongs to the superfamily of DEAD/H (Asp- Glu-Ala-Asp/His)-helicases [46-47] located in the N-terminal half of the proteins. In the C-terminal part, a HAND domain, a SANT domain and a juxtaposed SANT-like ISWI domain (SLIDE) are present. These domains are important for substrate recognition, they mediate interactions with the nucleosomal DNA as well as the histone core [48-50]. The SLIDE domain was found to mediate the DNA binding activity of ISWI. Deletion of either the SANT or SLIDE domains did not affect binding to nucleosomes, while deletion of both adversely affected binding. The "C" terminus of ISWI is therefore vital for nucleosome recognition. Deletion of SLIDE also largely abolished the ATPase activity of ISWI.

ISWI complexes participate in various biological functions, including chromatin assembly and nucleosome spacing, replication, transcriptional repression and activation [51, 52].

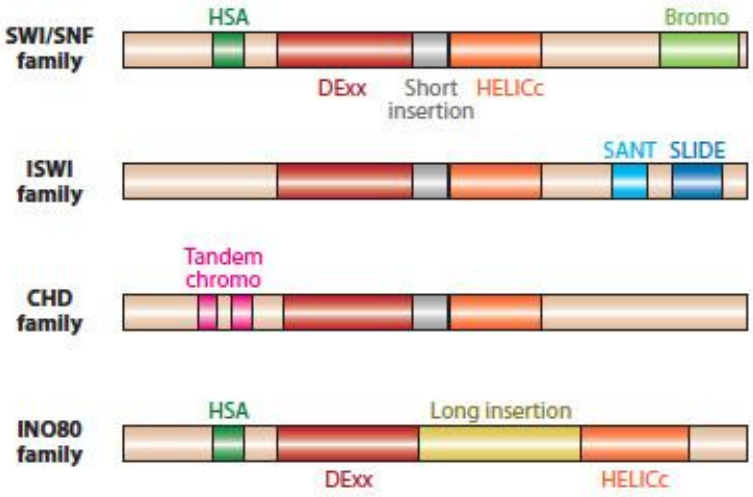

Figure 4: Remodeler Families, defined by their ATPase. All remodeler families contain a an ATPase domain that is split in two parts: DExx (red) and HELICc (orange). What distinguishes each family are the unique domains residing within, or adjacent to, the ATPase domain. Remodelers of the SWI/SNF, ISWI, and CHD families each have a distinctive short insertion (gray) within the ATPase domain, whereas remodelers of INO80 family contain a long insertion (yellow). Each family is further defined by distinct combinations of flanking domains: Bromodomain (light green) and HSA (helicase-SANT) domain (dark green) for SWI/SNF family, SANT-SLIDE module (blue) for ISWI family, tandem chromodomains (magenta) for the CHD family, and HSA domain (dark green) for the INO80 family. *Picture adpted from [53]*.

Multiple roles for the nucleosome remodeling ATPase ISWI

Transcription, replication, DNA repair, and other reactions involving chromatin substrates need to remove the chromatin barrier to allow regulatory proteins interaction with DNA. Nucleosome mobilization by chromatin remodeling complexes is an important mechanism by wich specific chromatin sites are made more accessible to regulatory factors [54].

ISWI chromatin remodelers can modify nucleosome position to block or clear promoters directly changing the expression level of the corresponding gene. These switch processes are triggered in the cell by different signals, such as hormone-dependent stimulation or metabolic changes. NURF, a chromatin remodeling complex that contains ISWI as ATPase subunit, was identified in *Drosophila* embryo extracts as a biochemical activity that alters nucleosome positioning at the hsp70 promoter in a GAGA factor-dependent manner [42, 43, 55]. NURF was subsequently shown to directly promote GAL4-mediated transcription from chromatin templates *in vitro* [56], providing one of the first indications that an ISWI complex can modulate gene activation in chromatin context. Instead, the ACF complex regulates cytokine expression in stimulated mouse [57], namely the expression of interleukin (IL)-2 and IL-3. The ACF complex binds to the corresponding gene loci before and after stimulation, and it induces IL-3 expression but reduces IL-2 expression.

The preferential association of ISWI with transcriptionally silent chromatin together with the changes in gene expression in *Drosophila ISWI* mutants, suggest that ISWI plays an important role also in transcriptional repression [58]. The *yeast* ISWI homologs Isw1 and Isw2

are subunits of multi-subunit complexes involved in transcription activation and repression [58]. The mammalian ISWI homolog, SNF2H, is part of the nucleolar remodeler NoRC complex, that has been shown to be involved in the repression of Pol I-dependent transcription [59]. Therefore, ISWI family complexes appear to both activate and repress transcription.

DNA replication is among the biological processes associated with extensive chromatin remodeling.

Studies in several model organisms have implicated ISWI in a variety of other nuclear functions including DNA replication [37] Interestingly, a chromatin-remodeling complex containing mammalian ISWI (Snf2h) and ACF1 (ACF1/BAZ1A/ WCRF180) is required to promote DNA replication through highly condensed heterochromatin in mammalian cells [60]. In contrast, the association of *Xenopus* ISWI (xISWI) with chromatin does not require ongoing DNA replication [37]. Furthermore, The *yeast* ISWI homologs Isw2 is enriched at the sites of active replication and helps facilitate replication fork progression [61]. The loss of ACF1 function in *Drosophila* shortens S phase [37]. These data indicate that remodeling complexes play a role in chromatin assembly and that, similarly to transcription, chromatin may present a barrier to DNA for factors engaged in replication. An ISWI complex may therefore assist the formation of nucleosomal arrays at the replication fork by virtue of its spacing activity.

ISWI complexes, by altering the structure or spacing of nucleosomes, appear to regulate chromosome structure. Several studies revealed a roles for ISWI in the generation or maintenance of higher-order chromatin structure. The first evidence of this role came from genetic studies in

Drosophila. Although *ISWI* is an essential gene in flies, individuals homozygous for *ISWI* null mutations survive until late larval development due to the high maternal contribution of ISWI [5]. The sever reduction in ISWI levels in the larval salivary gland of *ISWI* mutant larvae dramatically alters the appearance of the male X chromosome, causing it to appear much less compact than normally (see Figure 1) [5]. The condensation defects of male X chromosome in *ISWI* mutant larvae may reflect the ability of some ISWI-containing remodeling complexes to directly or indirectly influences higher-order chromatin structure. Genetic studies have demonstrated a specific ISWI containing complex, NURF, involvement in the regulation of higher-order chromatin structure. X chromosome defects indistinguishable from those observed in *ISWI* mutant larvae, are caused by mutations in *Nurf301*, the gene encoding the largest subunit of NURF [62]. Recent studies have revealed potential roles for other ISWI complexes including CHRAC and ACF in regulation of higher-order chromatin structure. The human complex RSF (Rsf1 / Snf2H) has been shown to maintain proper centromere structure by stabilizing the centromere protein A (CENP-A) histone variant at the centromeres [63]. Furthermore, RSF is required for normal mitotic progression. Snf2H is also present in a complex that loads cohesin onto mitotic chromosomes [61]. In *Xenopus*, the ISWI protein was found to be required for chromosome segregation [64], arguing for a conserved function of ISWIs in mitosis. The interaction between ISWI and members of the cohesin families has suggested novel mechanisms by which ISWI can regulate higher-order chromatin structure.

Aims of the study

Regulation of gene expression by ATP-dependent chromatin remodeling factors is one of the major mechanisms for controlling cell proliferation, differentiation and function [15]. Therefore, its easy to imagine how the modulation of chromatin structure and nucleosome positioning by ATP-dependent chromatin remodelers can contribute to aberrant gene expression of individual genes, that can lead to developmental abnormalities and diseases as cancer. Thus, understanding how the ATP-depentent chromatin remodeling complexes operate at molecular level and which genes they regulate is key to unraveling how the ATP-dependent chromatin remodelers interact with chromatin structure to regulate nucleare proceses as transcription.

During the three years of PhD my research was focused on the study of the ATP-chromatin remodeling factor ISWI and on its roles in chromatin compaction and transcription.

ISWI is the catalytic subunit of several ATP-dependent chromatin remodeling complexes (Table 1) [37]. ISWI is highly conserved during evolution and it is essential for cell viability [37].
Biochemical and genetic studies showed that ISWI complexes play central roles in gene expression and chromosome organization [40]. Particuly, in *Drosophila,* loss of ISWI function causes global transcription defects and leads to dramatic alterations in higher-order chromatin structure, including the apparent decondensation of both mitotic and interphase chromosomes [5, 65].
In the light of these existing data, the goal of this research project was to reveal the molecular basis of the interaction existing between the

evolutionary conserved ATP-dependent chromatin remodeling factor ISWI and the chromatin in the *Drosophila* genome.

In order to understand how ISWI regulate gene expression I looked at the systematic identification of ISWI chromatin binding targets, performing a genome-wide chromatin immunoprecupitation experiments.

To date, it is accepted the idea that altered modulation of chromatin structure and nucleosome positioning can contribute at deregulation of a variety of nuclear processes as transcription.
ISWI uses the energy of ATP hydrolysis to catalyze nucleosome spacing and sliding reactions [37] affecting chromatin structure.

Since the nucleosome remodeling activity of ISWI, my research project also had the aim of understand how the nucleosome spacing activity of ISWI can help to maintains an organized chromatin structure contributing at correct gene expression. Moreover, in order to understand how ISWI nucleosome remodeling activity influence gene expression and to clarify the correlation existing between binding and spacing ISWI activity, it was conducted a genome-scale identification of nucleosome positions in *wild type* and *ISWI* mutants. Moreover, another purpose of this analysis was to clarify the unusual chromosome condensation defects observed in *ISWI* mutants preferntialy on *Drosophila* male X chromosome [66]. Infact, the aberrant morphology of the male X chromosome in *ISWI* mutant larvae suggest some unique feature of the male X chromosome make it particulary sensitive to the loss of ISWI function.
Therefore this study was focused on explaining if global differences in nucleosome spacing are responsible for the male X chromosome condensation defects observed in *ISWI* mutants.

For this study the *Drosophila melanogaster* model organism was used as model system.

This study provided for the first time a genome-wide view of ISWI binding and nucleosome spacing activity in all *Drosophila* genome contributing a better knowledge of the molecular mechanism that is at basis of the ISWI activity in trasnscription regulation.

Experimental model

This study employed genetic, biochemical and bioinformatic approches using the fruit fly as model system.

Drosophila melanogaster was among the first organisms used for genetic analysis, and today it is one of the most widely used and genetically best-known of all eukaryotic organisms. All organisms use common genetic systems; therefore, comprehending processes such as transcription and replication in fruit flies helps in understanding these processes in other eukaryotes, including humans.

Drosophila melanogaster is one of the most studied organisms in biological research for several reasons. It is a small insect easily growing in the laboratory. It has a short generation time (about 10 days at room temperature), so several generations can be studied within a few weeks; has only four pairs of chromosomes: three autosomes, and one sexual pair. Its complete genome was sequenced and first published in 2000. Finally, the *Drosophila melanogaster* allows to study biological problems with both *in vivo* and *in vitro* studies.

Drosophila offers the rare advantage of visualizing interphase chromatin through light microscopic studies of large polytene chromosomes that are isolated from salivary gland nuclei of third-instar larvae (e.s Figure 1). Moreover, about 75% of known human disease-related genes have a recognizable match in the genome of fruit flies, and 50% of fly protein sequences have mammalian homologs. Therefore the small fruit fly can be used as a genetic model for several human diseases.

Results

ISWI binds chromatin near the Transcription Start Site

The normal growth, development and function of an organism require precise and coordinated control of gene expression and a correct chromatin organization. Deregulation of transcription or chromatin structure may result in the failure to expression genes responsible for cellular differentiation, or alternatively, in the transcription of genes involved in cell division perturbations, causing neoplasia [67]. This project was inspired by the idea that altered modulation of chromatin structure and nucleosome positioning from the ATP-dependent chromatin remodeler ISWI activity can contribute to aberrant gene expression and chromatin organization. Microarray studies revealed that ISWI is required for the proper expression of a large number of genes. Indeed, nearly 5% of the genes are altered in *ISWI* mutants, and 75% of these genes are expressed at higher levels, consistent with a predominant role for ISWI in transcriptional repression [66]. All date about ISWI function *in vivo* derives from studies conducted in *Drosophila* larval tissues [37]. Assuming a direct role of ISWI in the transcription regulation, a genome-wide identification of ISWI chromatin binding sites in larvae could provide some important insights in order to understand the transcription and chromosome condensation defects observed in *ISWI* mutants.

Therefore, to identify ISWI chromatin target sites across the *D.melanogaster* genome was performed a chromatin immunoprecipitation in larvae. Larval chromatin was immunoprecipitated (ChIPISWI) using the highly specific affinity purified anti-ISWI antibody and hybridized against the input chromatin on a set of tiled arrays covering the entire *Drosophila* genome with an average probe spacing of 100bp.

The ISWI enrichment over the fly genome was quantified using a "Peak Score*"* function that takes into account the "length" and "intensity" of the normalized raw $\log_2$(ChIPISWI/input) signals. Therefore, data derived from ChIP-on-chip analysis were expressed as peaks and every peak identifies an ISWI-enriched genomic region.

The analysis derived from ChIP-on-chip experiments identified 1,176 distinct ISWI-enriched chromatin regions corresponding to discrete ISWI peaks, mapping 925 unique gene loci and 141 intergenic regions with an average peak length of ~500 bp. Since, ISWI plays an important role in both transcriptional activation and repression [37] [68], were mapped ISWI binding sites relative to the Transcription Start Site (TSS) of genes present in the proximity of ISWI peaks. This analysis revealed that ISWI preferentially binds genes near their regulatory regions with an average peak at about 300bp downstream the TSS (Figure 5 A). Although, the majority of ISWI peaks maps in the proximity of the TSS (for specific examples see Figure 5 B-E) were also found the presence of many ISWI peaks at the level of exons, introns and at the 3'end of several genes *(data not shown)*.

ChIP-on-chip data on total larval chromatin were validated on salivary gland chromatin immunoprecipitated with the affinity purified anti-ISWI antibody [5] and analysed by semi-quantitative RT–PCR using specific primers for the representative ISWI-enriched regions identified in total larval chromatin (compare Figure 5 B and 5 E with Figure 6).

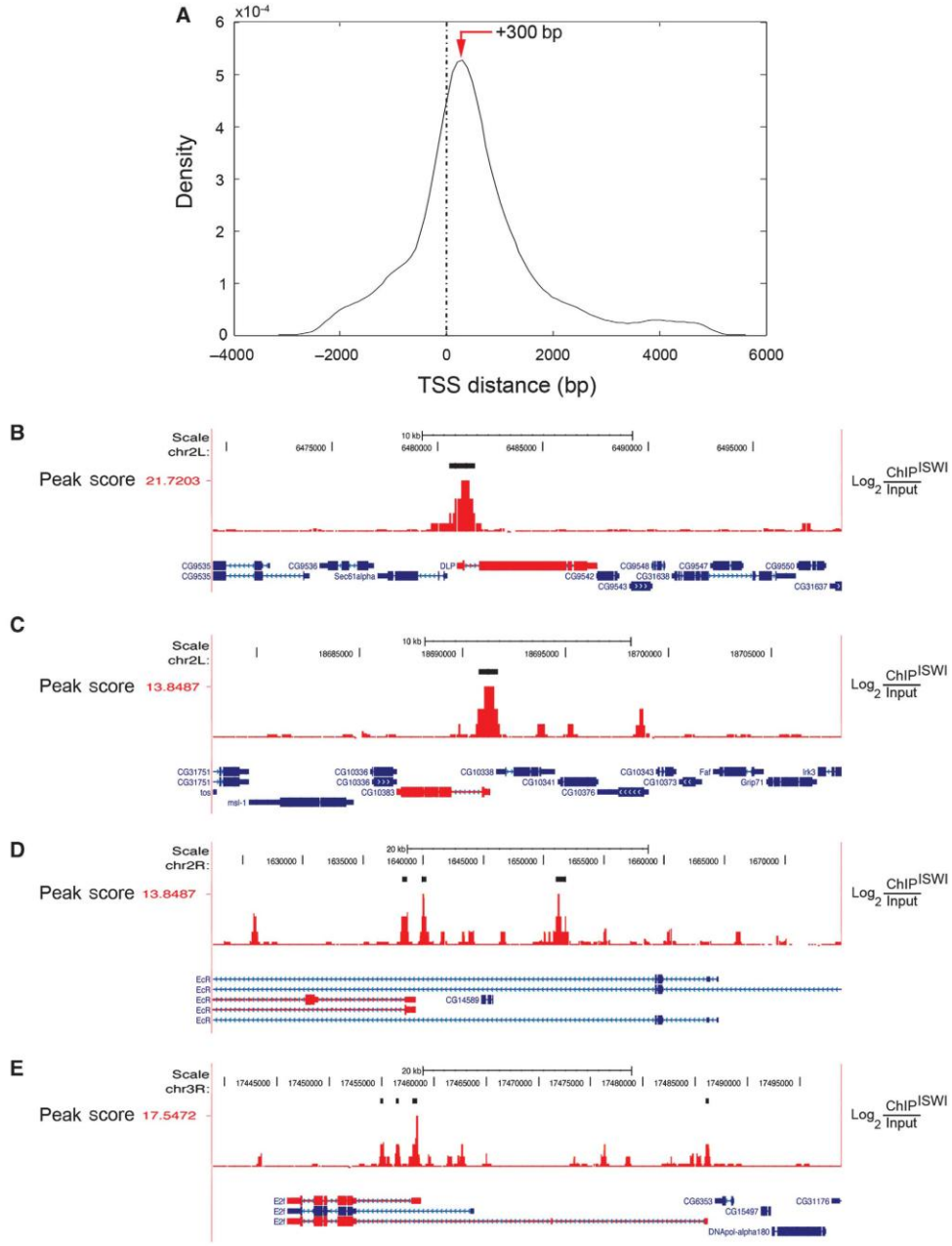

Figure 5: ISWI chromatin binding is enriched after the Transcription Start Site (TSS). **(A)** The density of ISWI-enriched genomic sequences was plotted relative to the distance from the TSS of nearby genes. **(B)** Representative example of a gene bound by ISWI at the level of the promoter–exon region. As expected, ISWI also binds genes whose expression is **(C)** increased or **(D)** decreased in *ISWI* mutant larval tissues relative to *wild-type* levels [66]. **(E)** ISWI binds near the TSS of genes involved in nurse cell apoptosis. ISWI enrichment is proportional to the normalized raw $\log_2$(ChIPISWI/input) red signals reported to the right y axis. The thick black bars highlight ISWI peaks. The peak score values of ISWI peaks are reported to the left y axis. Exons are represented by filled-in boxes, introns by a continuous line, while the 5' and 3' UTRs by thick lines. The transcription direction for each gene can be deduced by the repeated small blue arrows present in the intron segments. Genes bound by ISWI are shown in red.

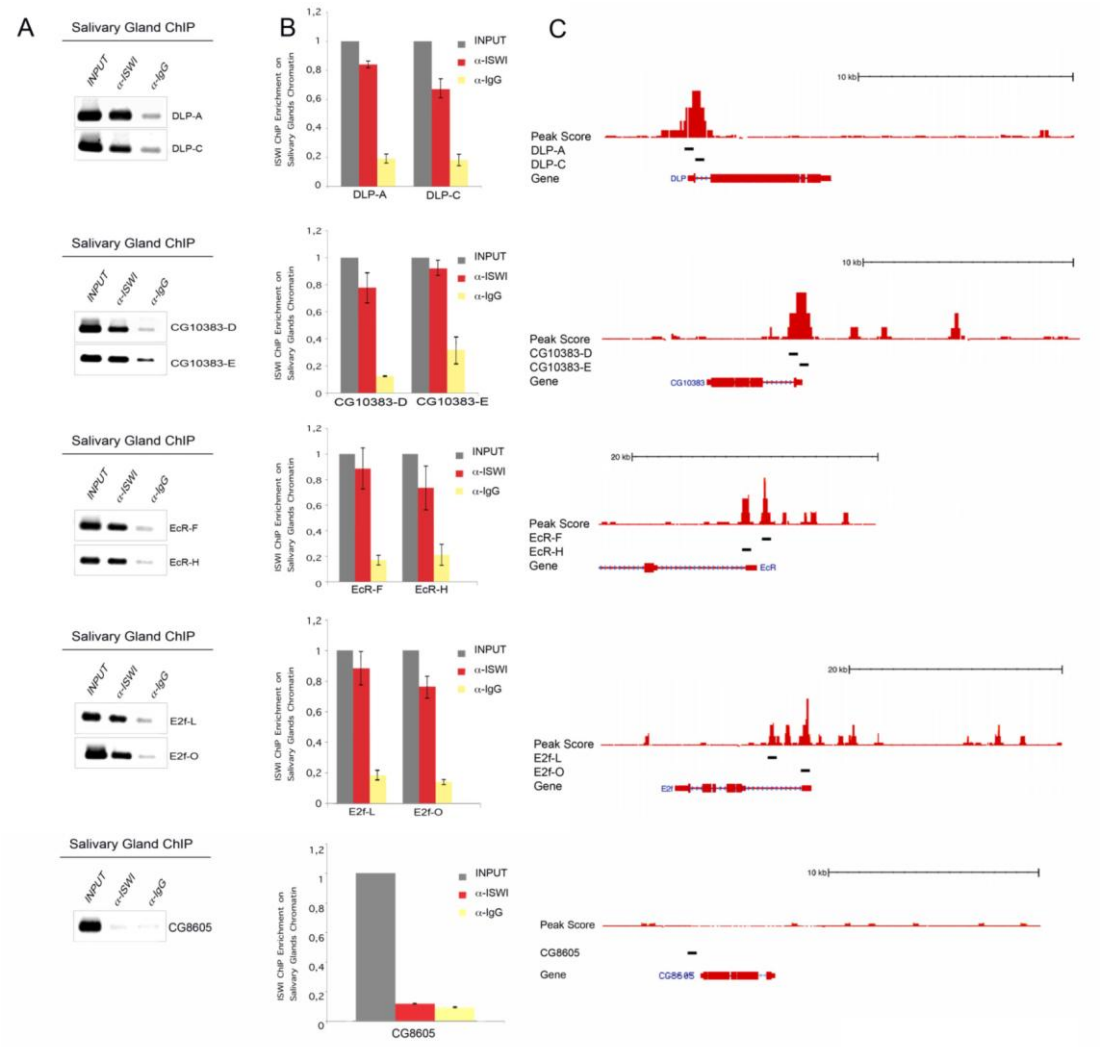

Figure 6: ISWI ChIP enrichment on salivary gland chromatin. (**A**) ISWI specific immunoprecipitated DNA was analyzed by semi-quantitative RT-PCR using specific primers for representative ISWI enriched chromatin regions identified by ChIP-on-chip on total larval chromatin (see genes in Figure 5B-E) as well as sites of low ISWI association (i.e. CG8605); the amplified regions are indicated by distinct capital letters. (**B**) Quantification of semi-quantitative RT-PCR experiments (shown in panel **A**). (**C**) Schematic graphic representation of the genomic regions amplified relative to the ISWI Peak Score and adjacent gene structures. ISWI-bound regions are represented by high Peak Score values.The short black bars indicate the genomic regions amplified. Exons are represented by filled-in boxes, introns by a continuous line, while the 5' and 3'-UTRs by thick lines. The transcription direction for each gene can be deduced by the repeated small blue arrows present in the intron segments.

Next, the ISWI binding sites near genes on the basis of their binding affinity to chromatin were mapped. For this purpose, the "Peak Score" values was used as an indirect measurement of ISWI chromatin binding strength/function and it was looked at the correlation existing between ISWI binding sites with higher Peak Scores values respect to gene

functional element (i.e. promoter, promoter-exon boundary, exon, exon-intron boundary, intron and intron-exon boundary). This analysis showed that only ISWI binding at the promoter-exon boundary regions tend to correlate with higher Peak Scores *(data not shown)*, strongly suggesting that the high density of ISWI-enriched chromatin regions near the promoter also correspond to sites were ISWI binds chromatin with higher affinity.

Collectively, this data suggest that in higher eukaryotes ISWI could regulate gene expression by remodeling chromatin near gene regulatory regions in the proximity of the TSS. Indeed, when were intersected genes whose expression changes at least 1.5-fold in *ISWI* mutant larvae, obtained from previous array expression data [66], with ISWI-bound genes, was found about the 50% of overlap (for specific examples, see Figure 5 C and D). However, this level of overlap dropped to 10% when were looked at genes which expression in *ISWI* mutant larvae change at least 4-fold [66]. Therefore ChIP data are the result of *bona fide* chromatin protein binding, array expression data underlie direct and indirect transcriptional effects caused by the loss of the chromatin protein studied. So, is possible that the two biological processes (binding versus activity) do not have to necessarily overlap.

ISWI binds several DNA consensus motifs on chromatin

In order to check if ISWI binds a particular group of genes involved in specific biological processes, was conducted an analysis of ISWI-bound genes based on their Gene Ontology (GO) classification. The GO analysis revealed that ISWI binds genes encoding for cellular and nuclear factors involved in a variety of biological functions (Figure 7 A) and that ISWI-bound genes are over represented in genes encoding factors involved in "Cellular Process" and in particular in "Nurse Cell Apoptosis" (Figure 7 B) (e.s. *E2f* ,Figure 5 E).

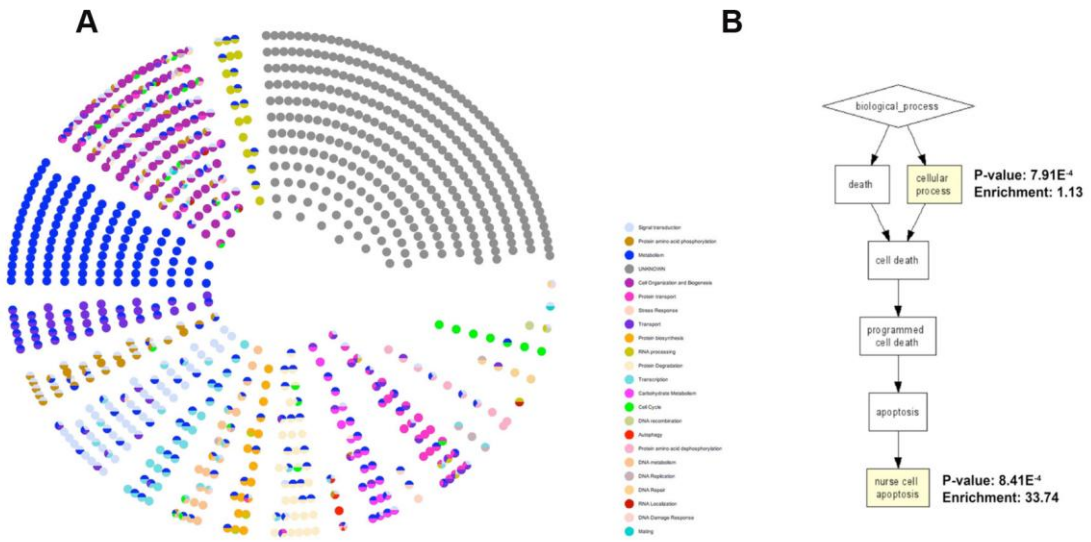

Figure 7: Gene Ontology analysis of genes bound by ISWI. (**A**) The 925 ISWI-bound genes are clustered in concentric circles and represented as nodes, colored according to their Gene Ontology (GO) categories as indicated in the legend. (**B**) Genes bound by ISWI were compared to all Drosophila genes and overrepresented GO terms were identified with Gorilla (http://cbl-gorilla.cs.technion.ac.il/). A corrected P-value threshold of 0.1 was used as a cut-off to report significant matches.

Until now was showed that ISWI binding near gene regulatory regions tend to correlate with higher peak score values. Given the high "peak score" values obtained for ISWI-binding sites near the TSS, it was also

reasoned that ISWI could preferentially bind specific DNA consensus motifs at the level of gene regulatory regions. Therefore, was used motif discovery scan (MDscan) [69], a robust motif discovery tool, to search for potential consensus ISWI–DNA interaction modules. This analysis resulted in the identification of a variety of IBE, corresponding to DNA sequence motifs associated directly or indirectly with ISWI in the context of chromatin. In particular, was found that ISWI binds several 4–5 letter IBE that are positively correlated with the 'peak score' function, strongly indicating that the identified motifs are likely associated with ISWI binding (Figure 8 A). Using multiple EM for motif elicitation (MEME), another motif searching algorithm [70], were identified similar IBE that contained a subset of the motifs found with MDscan (Figure 8 B–F).

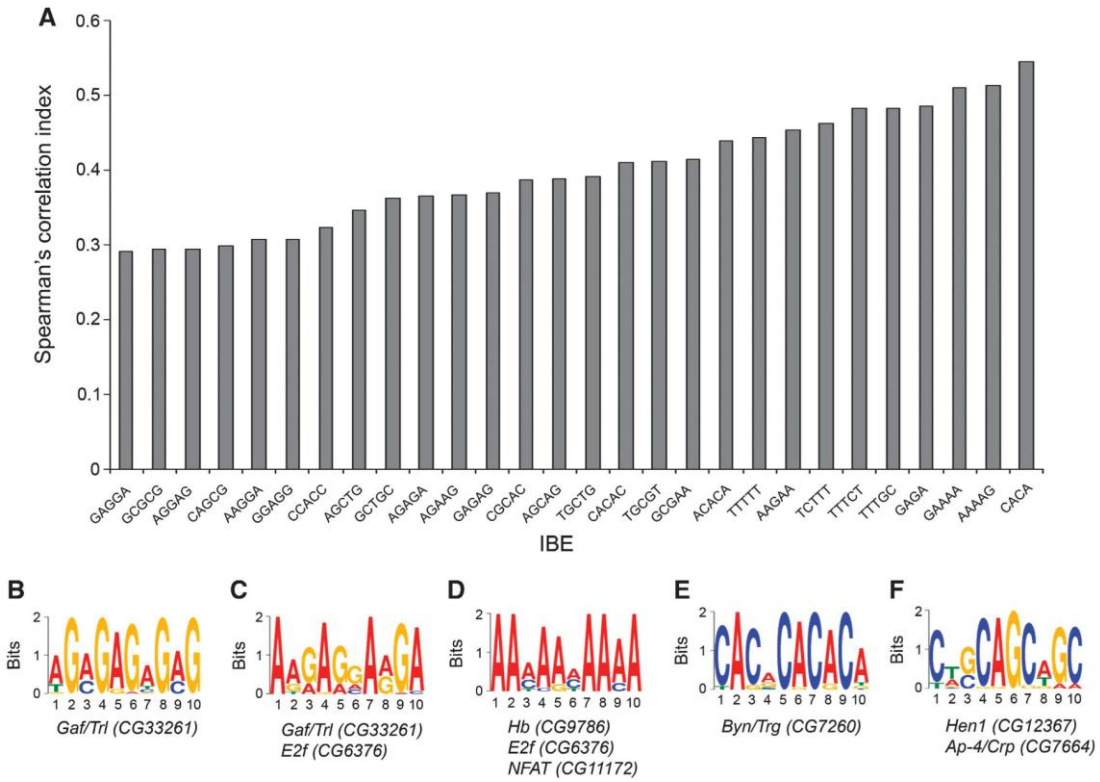

Figure 8: Identification of ISWI-binding elements (IBE). (A) DNA consensus motif corresponding to IBE identified with MDscan where correlated with the 'peak score' function using the Spearman's correlation index. **(B–F)** The top five motifs identified with multiple EM for motif elicitation (MEME) along with their putative D. melanogaster DNA-binding factors are shown. These logos are a graphical representation of DNA multiple sequence alignment. Each logo consists of a series of stacks of the four DNA deoxynucleotide (A, T, G, C), one

stack for each position in the sequence. The overall height of the stack indicates the sequence conservation at that position, while the height of symbols within the stack indicates the relative frequency of each nucleic acid at that position.

Interestingly, one of the top motifs identified with both algorithm corresponds to the GAGA factor (encoded by the Gaf/Trl gene) consensus sequence GAGAGA (Figure 8 B). The ISWI-containing multisubunit complex NURF was isolated based on its ability to recruit the GAGA factor to its target sites on chromatin *in vitro* [43]. In conclusion, the motif discovery analysis on ISWI-bound DNA sequences did not find a single consensus sequence but instead it allowed us to identify a collection of IBE that probably reflects the variety of factors that may recruits ISWI (i.e. GAGA factor), that are associated with it or that can be targeted to specific chromatin loci by the remodeling activity of ISWI.

ISWI remodels nucleosomes after the TSS

Collectively, ChIP-on-chip experiments revealed that ISWI binds its targets genes preferentially near the TSS, but this analysis did not tell us whether ISWI-enriched chromatin regions corresponded to active sites of chromatin remodeling. To answer this question and to determine if the transcription and chromosome condensation defects observed in *ISWI* mutant larvae could be directly correlated with ISWI chromatin remodeling alterations, was conducted a genome-wide identification of nucleosome spacing changes between *wild type* and *ISWI* mutant salivary gland chromatin (Figure 9). *Drosophila* salivary glands are actively transcribing interphase cells without division [71];[72]. Therefore, the salivary gland cells could be a good source of *Drosophila* chromatin, coming from an homogenous population of cells in interphase. Moreover, having a very high chromatin/cell ratio, salivary gland cells could have been an abundant source of nucleosomal DNA suitable for classic microarray-based identification of nucleosome positions [73].

Nucleosomal DNA (NucDNA) was isolated from *wild-type* and *ISWI* mutant male and female salivary gland cells, by digestion with micrococcal nuclease. NucDNA was purified and then was fluorescently labelled and competitively hybridized against total genomic DNA (GenDNA) on a custom-tiled array with a resolution of 20bp. A graph of $\log_2$(NucDNA/GenDNA) ratio values for spots along the chromosome showed nucleosomes as peaks about 140 base pairs long surrounded by lower ratio values corresponding to linker regions.

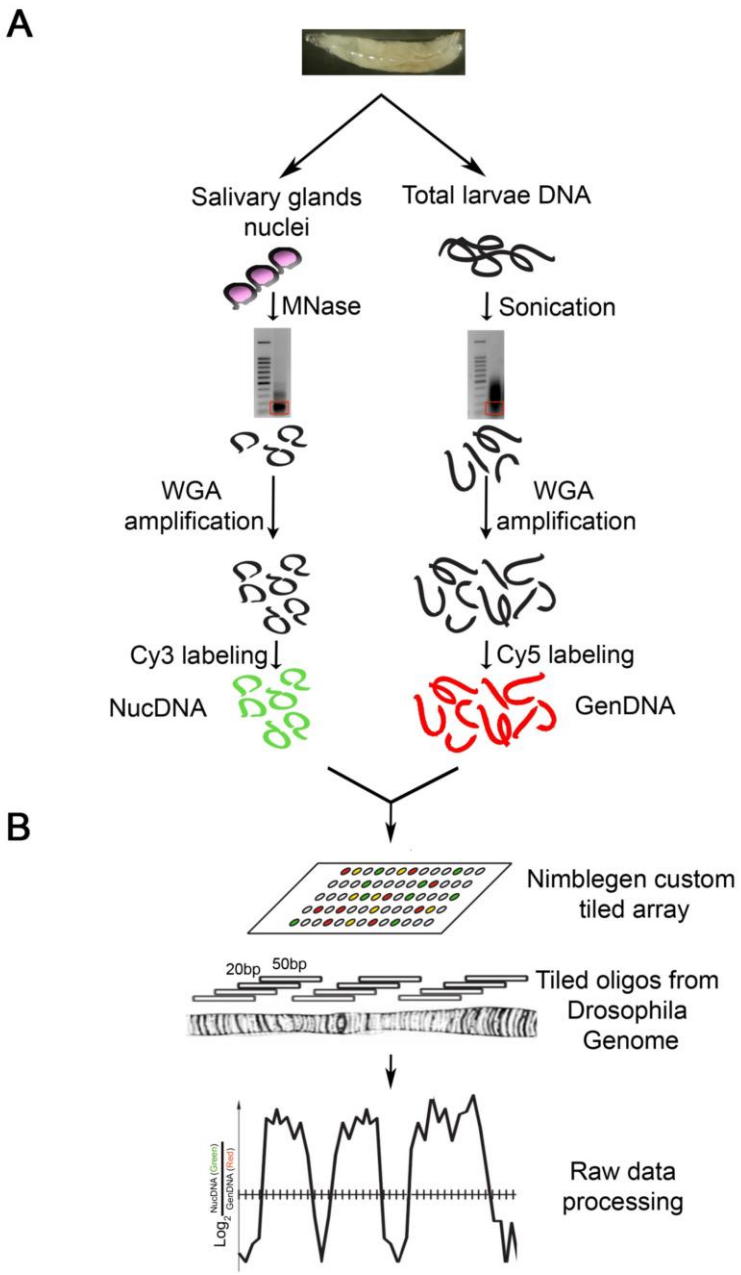

Figure 9: Experimental strategy to map nucleosome positions in *wild type* and *ISWI* mutant chromatin. (A) Chromatin from *wild type* or *ISWI* mutant male and female salivary gland cells was digested with Micrococcal Nuclease (MNase) to obtain nucleosomal DNA. The DNA from mononucleosomes (150bp; NucDNA) was purified from gel, amplified by Whole Genome Amplification (WGA) approaches, fluorescently labeled and finally competitively hybridized with sonicated genomic DNA (GenDNA) on a (**B**) custom tiled array of 50mers overlapped by 30bp covering the genomic regions of interest .The microarray-based method used allows the identification of nucleosomal and linker DNA sequences on the basis of susceptibility of linker DNA to micrococcal nuclease. The normalized $\log_2$(NucDNA/GenDNA) ratio signal shows nucleosomes as peaks surrounded by lower ratio values corresponding to linker regions [73].

Due to the restraint in the number of sequences that was possible print on a single chip, the array was designed to have some of the top ISWI-enriched sequences that were found by ISWI-ChIP. An equal number of DNA sequences corresponding to genes whose expression is altered in *ISWI* mutants [66] were also printed. Finally, were printed contiguous DNA sequences, equally distributed on the different *Drosophila* chromosomes and covering each nearly 1Mbp, encoding for genes not linked with ISWI functions (ISWI-binding or ISWI-dependent expression) and representing > 90% of genes present in the tiled array. The rational of such design was to have an array not biased on genomic sequences exclusively linked to ISWI function.

To measure nucleosome position on a higher eukaryote genome, that generates more complex and structured noise, that usually limits the identification of nucleosomal DNA, was used a recently algorithm called *Multi Layer Model* (MLM) developed in the Corona's lab [73]. One of the feature of the *MLM* is its ability to predicted nucleosomes with different mobility "features" which is typical of higher eukaryote chromatin [74]. In particular, the MLM can identify "Well Positioned" nucleosomes corresponding to nucleosome characterized by well defined peaks (bell shaped curve) covering about 150bp, "Delocalized" nucleosomes representing single nucleosomes or arrays of nucleosomes with high mobility, and finally "Fused" nucleosomes defining a single nucleosome that occupies two distinct close positions [74] (Figure 10 A).
When the MLM was applied to tiled array data did not were found significant differences in the global relative percentage of nucleosome mobility "features" existing between *wild type* and *ISWI* mutant salivary gland chromatin (Figure 10 B and C).

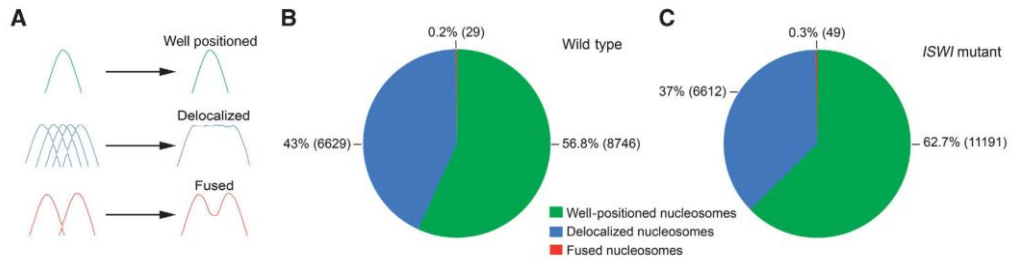

Figure 10: Multi Layer Model (MLM) nucleosome classification. (**A**) "Well positioned" nucleosomes (in green) are shown as peaks of a bell shaped curve, "Delocalized" nucleosomes (in blue) represent single nucleosomes or arrays of nucleosomes with high mobility, while "Fused" nucleosomes (in red) reflect a single nucleosomes that occupies two distinct close positions . On the left of the arrows are shown examples of nucleosome configuration that may contribute to the $\log_2$(Nuc DNA/GenDNA) ratio signal shape. The MLM detetected all three classes of nucleosomes with similar relative abundances between wild-type (**B**) and *ISWI* mutant (**C**) chromatin.

Thus, next the attention was focused to see at potential differences in nucleosome positioning near the TSS of all the genes present in the tiled array. As previously reported in other eukaryotes including flies, was found a well defined Nucleosome Free Region (NFR) mapping the TSS on all genes analyzed (Figure 11 A and C).

Interestingly, was also found one delocalized nucleosome preceding and two delocalized nucleosomes following the TSS in *wild type* chromatin (Figure 11 A and C). When then the 3'-end of the genes present in the tiled array were looked, was also found one delocalized nucleosome mapping the end of the transcripts (Figure 11 B and D). As showed in figure 10 E and F, when the analysis was extended to *ISWI* mutant chromatin, any significant difference in nucleosome positioning was observed respect to *wild-type* chromatin (Figure 11 A, B, E and F). However, when the attention was focused exclusively on ISWI-bound genes present in the tiled array, besides the NFR mapping at the TSS, and the delocalized nucleosome preceding the TSS, two well-positioned

nucleosomes following the TSS in *wild type* chromatin were found (Figure 12 A).

Remarkably, these two well-positioned nucleosomes present in ISWI-bound genes after the TSS become delocalized in *ISWI* mutant chromatin (Figure 12: compare C and E).

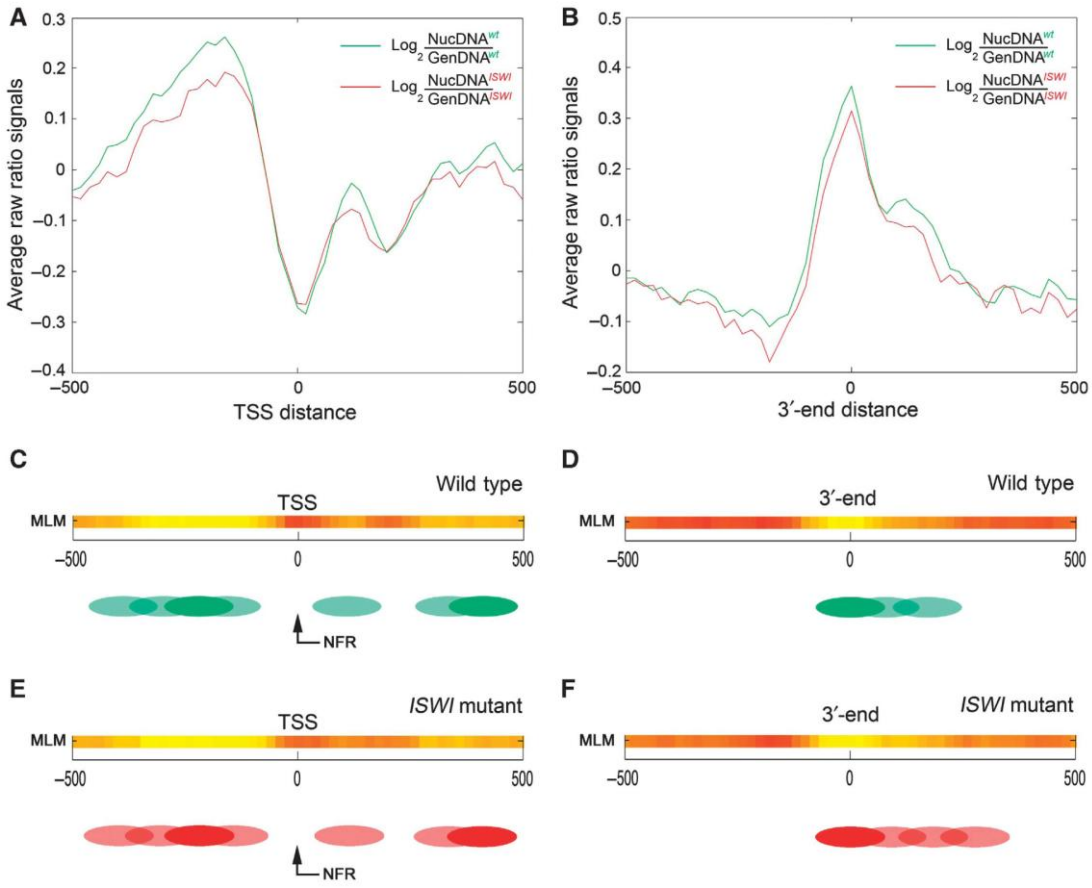

Figure 11: Differences in nucleosome positioning around the TSS and 3'-end between *wild-type* and *ISWI* male chromatin. The average $\log_2$(NucDNA/GenDNA) raw ratio of all the signals coming from *wild-type* (green) and *ISWI* mutant (red) male salivary gland chromatin of all genes present in the nucleosome-tiled array was plotted relative to the **(A)** TSS distance or the **(B)** 3'-end distance. Nucleosome positions were calculated with the MLM for **(C)** *wild-type* and **(E)** *ISWI* mutant chromatin near the TSS, and for **(D)** *wild-type* and **(F)** *ISWI* mutant chromatin around the 3'-end. The MLM analysis shows well-positioned nucleosomes as shadings of yellow, linker regions in red, while delocalized nucleosomes in orange. The green and red ovals represent an interpretation of the MLM nucleosome positioning analysis in *wild-type* and *ISWI* mutant chromatin, respectively. Filled ovals indicate well-positioned nucleosomes, while shaded ovals show delocalized nucleosomes.

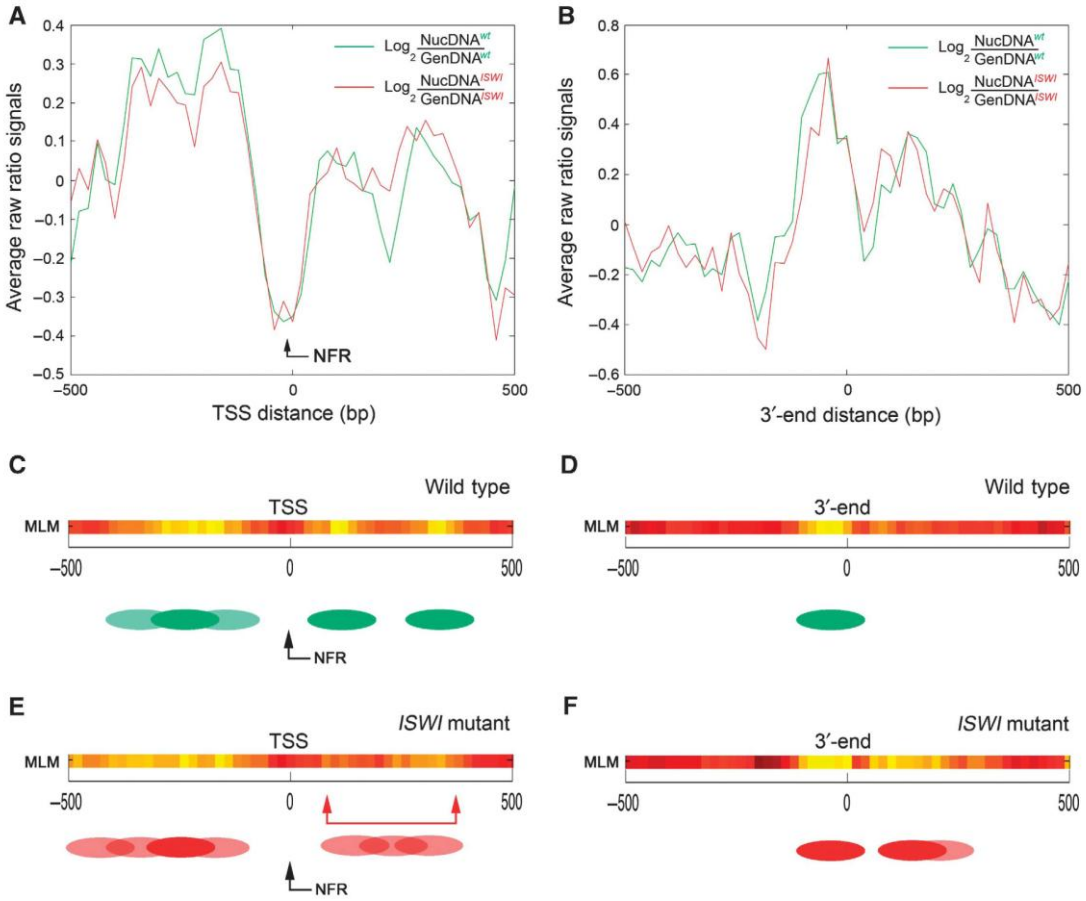

Figure 12: Loss of ISWI causes nucleosome spacing defects after the TSS on ISWI-bound genes. The average $\log_2$(NucDNA/GenDNA) raw ratio of the signals coming from *wild-type* (green) and *ISWI* mutant (red) male salivary gland chromatin of all ISWI-bound genes present in the nucleosome positioning array was plotted relative to the **(A)** TSS distance or the **(B)** 3'-end distance. The nucleosome-free region (NFR) mapping the TSS is indicated by the black arrow. Nucleosome positions were calculated with the MLM for **(C)** *wild-type* and **(E)** *ISWI* mutant chromatin relative to the TSS, and for **(D)** *wild-type* and **(F)** *ISWI* mutant chromatin around the 3'-end. The MLM analysis showed well-positioned nucleosomes as shadings of yellow, linker regions in red, while delocalized nucleosomes in orange. The green and red ovals represent an interpretation of the MLM nucleosome positioning analysis in *wild-type* and *ISWI* mutant chromatin, respectively. Filled ovals indicate well-positioned nucleosomes, while shaded ovals show delocalized nucleosomes. The double-arrowed red bar indicates the region after the TSS where was observed higher nucleosome mobility in the absence of ISWI.

Similarly, the nucleosome mapping at the 3'-end also showed a tendency to delocalize in *ISWI* mutant when compared to *wild type* chromatin (Figure 12: compare D and F). Collectively, the nucleosome position data support a role for ISWI in organizing nucleosome positions after the TSS of ISWI-bound genes.

As mentioned, microarray studies revealed that ISWI is required for the proper expression of a large number of genes [66]. However, was reasoned that the changes in nucleosome positions that were observed can be due to the indirect effects of changes in transcription in the ISWI mutant. Therefore, were looked at a possible correlation existing between changes in transcription levels and nucleosomes positions in the *ISWI* mutant, based on published genome-wide transcriptome array data [66] as well as on new RT–PCR data. Among ISWI-bound genes with changes in nucleosome positioning, were found without distinction both an increase or a decrease in transcription *(data not shown)*. In conclusion, comparing *wild-type* and *ISWI* mutants any positive or negative correlation between changes in transcription levels and nucleosomes positions in ISWI-bound or not- bound genes was observed. Nevertheless, not be excluded that the changes in nucleosome positions observed could be in part indirectly caused by changes in transcription resulting from loss of ISWI function.

ISWI modulates nucleosome positions in gene regulatory regions of dosage compensated genes in both males and females

Apart from its role in transcription regulation, ISWI also plays an important global function in the regulation of higher-order chromatin structure *in vivo*. Loss of *ISWI* in larval salivary gland cells leads to the dramatic decondensation of the male X chromosome [5]. In order to explorer the possibility that the male X chromosome condensation defects observed in *ISWI* mutants could be caused from global differences in nucleosome spacing, were mapped the differences in nucleosome positioning between *wild-type* and *ISWI* mutant male and female salivary gland chromatin. Using the normalized raw $\log_2$(NucDNA/GenDNA) ratio signals or the MLM-calculated nucleosome positions (on ISWI-bound and not-bound chromatin regions), were found many sites of altered nucleosome positioning between *wild-type* and *ISWI* mutant chromatin (Figure 13 A and B). Interestingly, these nucleosome differences also tend to globally accumulate near the TSS, but how showed in Figure 13 A and B, the peak values do not match the gene intervals where were observed the major changes in nucleosome positions in ISWI-bound genes (see the red arrows on Figure 13 A and B and compare it with the red double-arrowed bar on Figure 12 E). Surprisingly, then mapping the genic and intergenic differences on each *Drosophila* chromosomes, was not detected a significant enrichment in the relative abundance of nucleosome spacing differences for the X chromosome or any particular chromosome arm (Figure 13 C and D). Therefore this analysis suggested that ISWI chromosome condensation defects are not correlated with global ISWI-dependent nucleosome spacing changes.

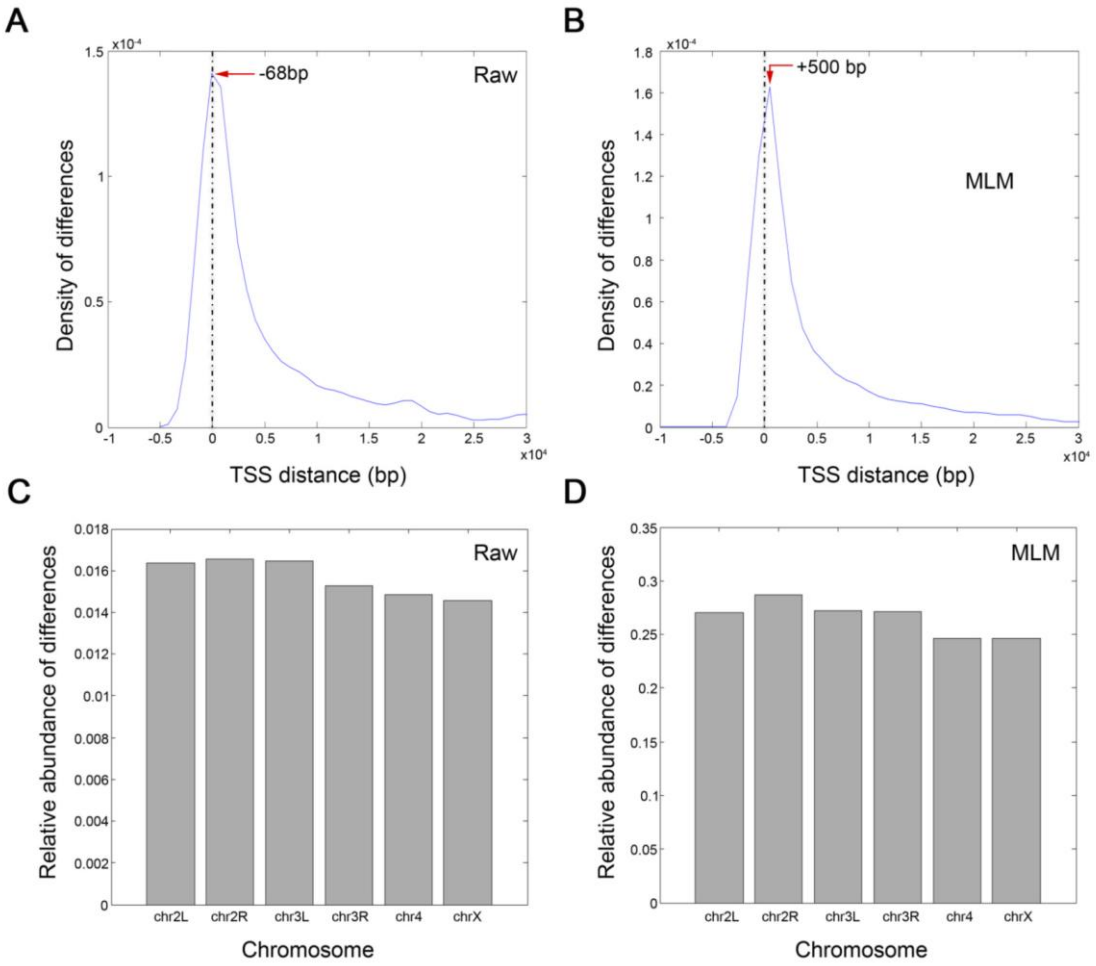

Figure 13: Mapping of nucleosome position differences between *wild type* and *ISWI* mutant chromatin. The density of nucleosome positioning changes occurring between *wild type* and *ISWI* mutant chromatin was calculated using the **(A)** normalized raw log2(NucDNA/GenDNA) ratio signal or **(B)** the MLM and was plotted relative to distance from the Transcription Start Site (TSS) of nearby genes. The red arrows indicate the peak distance from the TSS of the density distribution. The normalized relative abundance of nucleosome positioning changes occurring between *wild type* and *ISWI* mutant chromatin,using the **(C)** normalized raw $\log_2$(Nuc DNA/GenDNA) ratio signal or **(D)** the MLM, was calculated for each chromosome arm

Subsequently was considered the possibility that 90% of sequences with low frequency of ISWI association present in the nucleosome positioning array (for simplicity from now on referred as not bound), can mask the nucleosome spacing differences occuring in the ISWI-bound sequences. Then, the attention was focused only on nucleosome position changes existing in ISWI-bound genes between *wild type* and *ISWI* mutant chromatin. Using normalized raw $\log_2$(NucDNA/GenDNA) ratio signals

and the MLM calculated nucleosome positions, was found that nucleosome position differences in ISWI-bound genes map after the TSS where were observed the major changes in nucleosome spacing in ISWI-bound genes (see red arrows in Figure 14 and compare it with the red double arrowed bar on Fig.12 E).

Interestingly when were mapped the differences in nucleosome positioning in ISWI-bound genes for each chromosome arm, as is showed in figure 14 C and D, they tend significantly to accumulate on the male X chromosome respect to all ISWI-bound genes analysed as well as the female X chromosome (Figure 14 C). One easy way to explain the male X chromosome tendency to accumulate differences in nucleosome positions is that ISWI is enriched on genes mapping the X chromosomes. Indeed, ISWI binds genes on the X with a statistically significant higher frequency (Figure 14 D).

Sex chromosomes in flies, like in many eukayotes, undergo the process of dosage compensation. Dosage compensation is the mechanism by which X-linked gene expression levels are equalized between XX and XY organisms. In *D. melanogaster,* dosage compensation takes place in the XY male by an approximate two fold upregulation of X-linked genes. The dosage compensation is dependent on a multisubunit complex (MSL) that is specifically targeted to the male X chromosome, leading to the acetylation of dosage compensated genes in lysine 16 of histone H4 (H4K16Ac) by the MOF histone acetyltransferase [75]. This histone modification is thought to increase by two fold the transcription of dosage compensated genes, thus compensating for the presence of one X chromosome in males [76]. Remarkably, when were compared the ISWI binding genes with genes strongly-bound and ones weakly-bound by the dosage compensation complex [77] was found a strong enrichment of

ISWI binding on or near genes strongly-bound by dosage compensated complex. Therefore, were analyzed the differences in nucleosome positions existing in genes strongly (MSL-bound) and weakly bound (MSL-not bound) by the dosage compensation complex, present in the nucleosome position array, and the effect of *ISWI* loss on those genes.
This analysis showed that ISWI-bound genes strongly bound by the dosage compensation complex present on average a well-positioned nucleosome before a nucleosome-free TSS (Figure 14 E). On the other hand, several delocalized nucleosomes occupy the TSS of ISWI-bound genes weakly bound by the dosage compensation complex (MSL not bound) on the X chromosome (Figure 14 F). Similarly, when were analysed nucleosome positions in *wild-type* female chromatin, were found a nucleosome positions around the TSS very different from those found in all ISWI-bound genes *(data not shown).*

The nucleosome position compare between ISWI-bound genes strongly and weakly bound by the dosage compensation complex mapping on the X chromosome showed a very peculiar nucleosome organization at the level of their TSS (absence of NFR) in both males and females. Probably, in the absence of dosage compensation on both males and females, this nucleosome organization is functional to a specific transcriptional regulation of those genes.

As showed in Figure 14 F and H, while the loss of *ISWI* has little effect on genes weakly bound by the dosage compensation complex (compare Figure 14 F and 14 H), the TSS of genes strongly bound by the dosage compensation complex becomes occupied by a delocalized nucleosome in the absence of *ISWI* (compare Figure 14 E and 14 G).
However, the nucleosome position changes resulting from ISWI loss at the 3'-end of dosage compensated genes and in genes with low frequency

of association with the dosage compensation complex, showed that loss of ISWI had little effect *(data not shown)*. Moreover, in the female chromatin, was observed that changes in nucleosome positions around the TSS of MSL-bound genes were very different from those found in males. Remarkably, those changes did not affect the nucleosome-free TSS *(data not shown)*. Collectively, all this data indicate that ISWI binding on the X-linked genes causes specific nucleosome changes in both male and female chromatin.

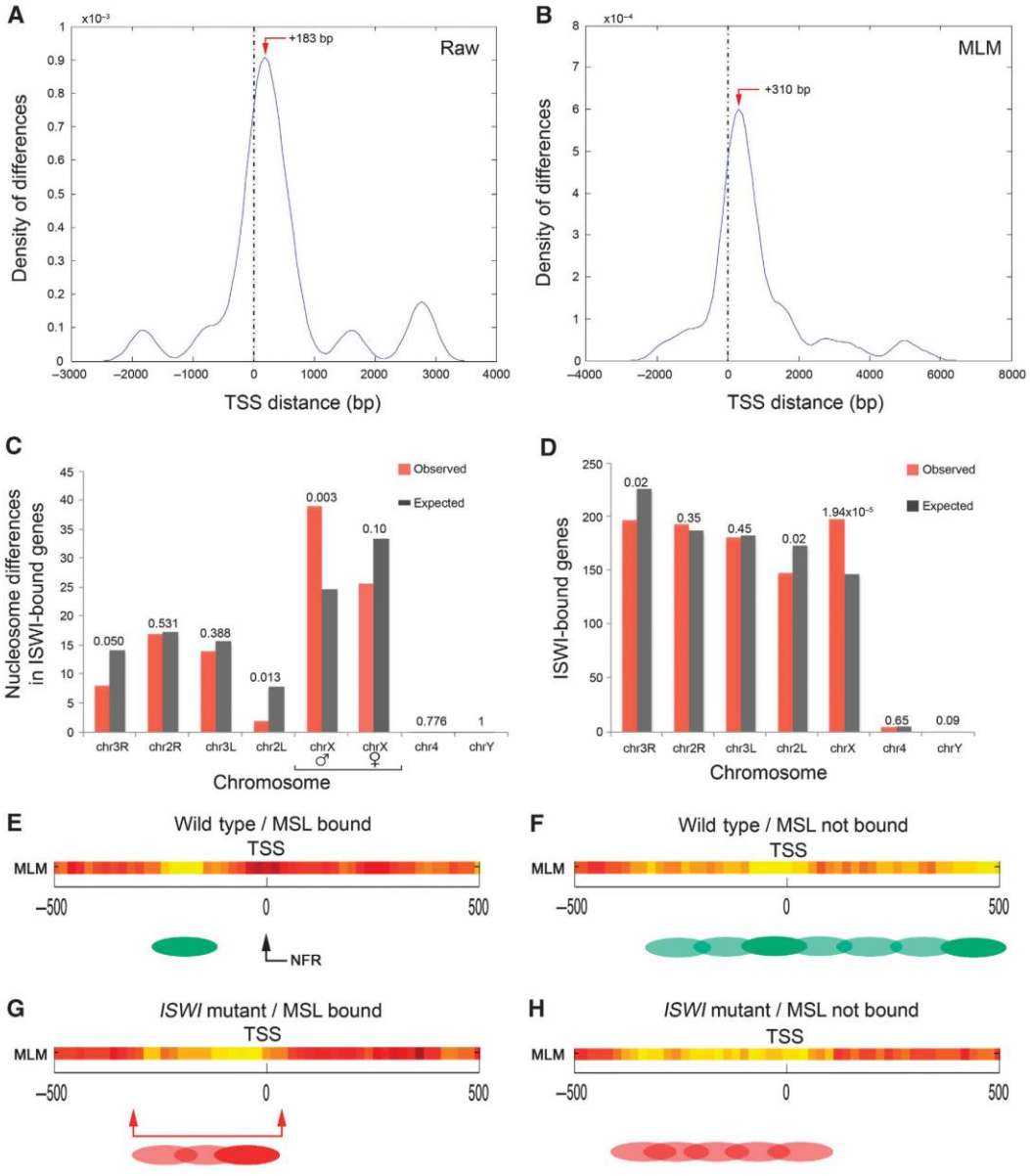

Figure 14: ISWI binds dosage compensated genes to make their TSS nucleosome free.

The density of nucleosome positioning changes occurring between *wild-type* and *ISWI* mutant chromatin was calculated using the **(A)** normalized raw $\log_2$(NucDNA/GenDNA) ratio signal or **(B)** the MLM, and was plotted against the distance from the transcription start site (TSS) of ISWI-bound genes. The red arrow indicates where the nucleosome difference density peaks relative to the TSS. **(C)** Nucleosome position differences between *wild-type* and *ISWI* mutant chromatin for all ISWI-bound genes were calculated for each chromosome arm and plotted against their expected values, based on the relative representation of the different chromosome sequences in the nucleosome-tiled array. **(D)** The number of ISWI-bound genes for each chromosome arm was calculated and plotted against their expected values, based on the known number of genes mapping each chromosome. The P-values calculated comparing the expected with the observed values are shown on top of each histogram pair. Nucleosome positions were calculated with the MLM for **(E)** *wild-type* and **(G)** *ISWI* mutant chromatin relative to the TSS of ISWI- and MSL-bound genes, and for **(F)** *wild-type* and **(H)** *ISWI* mutant chromatin relative to the TSS of genes not bound neither by ISWI nor MSL. The MLM analysis shows well-positioned nucleosomes as shadings of yellow, linker regions in red, while delocalized nucleosomes in orange. The green and red ovals represent an interpretation of the MLM nucleosome positioning analysis in *wild-type* and *ISWI* mutant chromatin, respectively. Filled ovals indicate well-positioned nucleosomes, while shaded ovals show delocalized nucleosomes. The black arrow indicates the nucleosome-free region at the TSS of *wild-type* ISWI- and MSL-bound genes. The red double-arrowed bar indicates the region at the TSS where was observed nucleosome occupancy in the absence of ISWI in ISWI- and MSL-bound genes.

Discussion

The accurate preservation of genetic information is crucial for all living organisms [78]. In eukaryotes, whether single-celled yeast or complex mammals, the DNA containing the genetic information is wrapped around beads of histone proteins to form structures called nucleosomes along the length of the DNA. This packaging let the cell organize its large and complex genome into the nucleus, but also prevents the access to DNA of proteins involved in the regulation of all nuclear processes [14]. These notions are all recognized by the scientific world, as well as that the eucaryotes have evolved regulatory mechanisms to induce structural changes to chromatin in response to environmental and cellular stimuli. The ATP-dependent chromatin remodeling complexs are one classes of enzymes that modulate chromatin accessibility[11].

During my years of PhD my research was focused on the evolutionarily conserved ATP-dependent nucleosome remodeling factor ISWI and on its role in gene regulation and chromatin organitation in the *Drosophila* genoma.

The *Drosophila* ISWI protein functions as ATPase subunit of several nucleosome remodeling complexes, including CHRAC, ACF and NURF [52]. ISWI can space nucleosomes affecting a variety of nuclear processes as DNA replication, RNA transcription and chromosome organization [37]. Particularly, in *Drosophila* loss of *ISWI* function causes global transcription defects and leads to the dramatic alterations of higher-order chromatin structure, especially on the male X chromosome [37]. As was showed before, this work wanted to investigate how the ISWI activity can influence chromatin condensation and gene expression genome-wide in higher eukaryotes. In order, to answer this questions was performed a genome-wide identification of ISWI chromatin-binding sites and

nucleosome spacing activity in the higher eukaryote *Drosophila melanogaster*.

The results of this study showed that ISWI binds both genic and intergenic regions. In particular, ISWI binds genes near their promoters.
Intersecting ISWI chromatin binding and nucleosome position dataset was possible to see that ISWI bound genes present specific alterations in nucleosome positioning at the level of the Transcription Start Site, providing an important insights in understanding ISWI role in higher eukaryote transcriptional regulation.
Moreover, thank a robust motif discovery analysis on ISWI-bound DNA sequences was possible to identify a collection of ISWI-binding elements (IBEs) that probably reflects the variety of factors that may recruits ISWI (Figure 2 B–F), that are associated with it or that can be targeted to specific chromatin loci by the remodeling activity of ISWI.

Finally, the last part of this work was focused to understand the nature of male X chromosome condensation defects observed in ISWI mutants [66]
.
The unusual sensitivity of the male X chromosome to the loss of ISWI function has suggested in the past that changes in chromatin structure that accompany dosage compensation might regulate the ability of ISWI to remodel chromatin *in vivo*. Indeed, dosage compensation is necessary and sufficient for the chromosome defects observed in *ISWI* mutant larvae [79]. In particular, genetic studies have shown that in the absence of ISWI the decondensed male X chromosome is dosage compensated and that *in vitro* H4K16Ac counteracts ISWI nucleosome spacing activity by reducing ISWI binding to chromatin [17, 79]. However, the data obtained with this work showed that ISWI binds dosage compensated genes

affecting nucleosome positioning near the TSS. Interestingly, it has been recently shown that the dosage compensation complex preferentially binds its target genes towards their 3'-end [77]. When were mapped ISWI binding on MSL-bound genes, was found that ISWI tend to bind the 5'-end on those genes *(data not shown)*. Therefore, ISWI and the MSL occupy complementary gene functional elements along dosage compensated genes, making the observation on nucleosome changes obtained in this work consistent with published data.

In conclusion, this work demostrated that the loss of ISWI globally causes subtle changes in nucleosome positioning. However, these changes are highly localized and mainly concentrated at level of the TSS, including the ones mapping the X chromosome that are particularly enriched in dosage compensated genes, probably explaining the specific sensitivity of the male X for ISWI loss [5, 79].

Although this data suggest that in higher eukaryotes ISWI could regulate gene expression by remodeling chromatin near gene regulatory regions, additional studies will be necessary to understand the advantage of having ISWI-sensitive-nucleosome-free TSS on dosage compensated genes. Furthermore, the genome-wide analysis of ISWI binding and nucleosome spacing activity in *Drosophila* also revealed that ISWI-dependent alterations in nucleosome positioning at the level of the TSS are unlikely to be correlated with global chromatin structural alterations observed when ISWI activity is lost. Collectively, this work provided new insights on the role played by the evolutionarily conserved chromatin remodeling factor ISWI in transcriptional regulation and chromosome organization in higher eukaryote

Materials and Methods

Drosophila stocks and genetic crosses

Flies were raised at 25°C or 18°C on K12 medium (USBiological). Unless otherwise stated, strains were obtained from Bloomington Stock Center and are described in FlyBase (http://www.flybase.org). For nucleosomal and genomic DNA preparation $ISWI^1/ISWI^2$ male larvae were obtained as previously described [80].

Larval chromatin preparation

For each experiment about 2gr of *wild-type* third-instar larvae were collected, quickly frozen in liquid nitrogen and ground to powder. Samples were rapidly homogenized with a Douncer in 20ml of 1XPBS and fixed for 20 minutes at room temperature with 540µl of 37% formaldehyde (SIGMA). The cross-linking was stopped by incubating for 5 minutes with 1ml of 2.5M Glycine. Nuclei were collected by centrifugation at 1,600g for 5 minutes at 4°C and washed 3 times in 1XPBS. The nuclear pellet was resuspended in Nuclear extraction buffer (15mM Hepes, pH 7.0, 5mM MgCl2, 0.2mM EDTA, 0.5mM EGTA, 10mM KCl, 350mM Sucrose, 0.1% Tween, 1mM DTT, 1X protease inhibitors cocktail-Roche, 0.5mM PMSF) and centrifuged at 3,220g for 5 minutes at 4 °C. The pellet was resuspended in RIPA 150 (50mM Tris-HCl, pH 8.0, 1% Triton X-100, 2mM EDTA, pH 8.0, 150mM NaCl, 0.1% sodium deoxycholate, 0.2% SDS, 1mM DTT, 1X protease inhibitors cocktail-Roche, 0.5mM PMSF) and sonicated for 5 min (60s on, 30s off) at the maximum power, keeping samples on ice. The sheared chromatin solution (with an average length of ~500-1000bp) was clarified by centrifugation at 10,000g at 4oC for 15 minutes. The supernatant was collected, quickly frozen in liquid nitrogen, and stored at -80°C.

Salivary glands chromatin preparation

Fifty *wild-type* salivary glands were dissected in DMM medium [81] and were fixed for 5 min at room temperature in 240µl of fixing solution (10mM HEPES, pH 7,6, 25mM KCl, 5mM MgCl2, 5% glycerol, 2% formaldehyde). The cross-linking was stopped by incubating for 2 minutes with 1ml of 125mM Glycine. Salivary glands were transferred in eppendorf containing 100µl of M buffer (10mM HEPES, pH 7,6, 25mM KCl, 5mM MgCl2, 5% glycerol, 1mM PMSF, 1mM DTT) and were kept on ice. Nonidet-P40 was added to a final concentration of 0.5% and the mix was homogenized with 50 strokes using a plastic pestel on ice. Samples were centrifuged at 2,100g for 5 minutes at 4°C to pellet nuclei. The nuclear pellet was washed three times in 25 µl of PBS 1X supplemented with PMSF. The nuclear pellet was resuspended in 250µl of nuclear extraction buffer (15mM Hepes, pH 7.0, 5mM MgCl2, 0.2mM EDTA, 0.5mM EGTA, 10mM KCl, 350mM Sucrose, 0.1% Tween, 1mM DTT, 1X protease inhibitors cocktail-Roche, 0.5mM PMSF) and centrifuged at 3,220g for 5 minutes at 4 °C. The pellet was resuspended in 250µl of RIPA 150 (50mM Tris-HCl, pH 8.0, 1% Triton X-100, 2mM EDTA, pH 8.0, 150mM NaCl, 0.1% sodium deoxycholate, 0.2% SDS, 1mM DTT, 1X protease inhibitors cocktail-Roche, 0.5mM PMSF) and sonicated (four times 30s on, 30s off) at the maximum power, keeping the samples on ice. The sheared chromatin solution (with an average length of ~500-1000bp checked by EtBr stained agarose gel electrophoresis) was clarified by centrifugation at 10,000g at 4oC for 5 minutes. The supernatant containing the fixed and sheared chromatin in solution was collected, quickly frozen in liquid nitrogen, and stored at -80°C.

ISWI Chromatin immunoprecipitation (ChIP)

Chromatin was diluted 1:1 in ChIP dilution buffer (16.7 mM Tris-HCl, pH 8.0, 1.2 mM EDTA, 167 mM NaCl, 0.01% SDS, 1.1% Triton X-100, 1X protease inhibitors cocktail- Roche). 1ml of diluted chromatin was incubated with 1µg of affinity purified anti-ISWI [5] antibody overnight at 4 ^{o}C on a rotating wheel. A 10µl aliquot corresponding to 1% of diluted chromatin was taken as input. Immunocomplexes were recovered by incubation with 60µl of Protein A/G Plus-Agarose (Santa Cruz Biotech) for 1h at 4oC. The Protein A/G Plus-Agarose beads were washed for 5 min at 4oC with 1ml of the following buffers: two washes with Low salt buffer (20 mM Tris-HCl, pH 8.0, 2 mM EDTA, 150 mM NaCl, 0.1% SDS, 1% Triton X-100), one wash with High salt buffer (20 mM Tris- HCl pH 8.0, 2 mM EDTA, 500 mM NaCl, 0.1% SDS, 1% Triton X-100), one wash with LiCl buffer (10 mM Tris-HCl, pH 8.0, 1 mM EDTA, 0.25 M LiCl, 1% NP-40, 1% deoxycholic acid) and finally two washes with TE buffer (10 mM Tris-HCl, pH 8.0, 1 mM EDTA pH 8.0). The immunocomplexes were eluted by two sequential incubations in 100 µl of Elution buffer (1% SDS, 0.1 M sodium bicarbonate) for 15 minutes at room temperature. The formaldehyde cross-link was reversed by incubating samples with 20µl 5M NaCl at 65°C overnight. The immunoprecipitated and reverse cross-linked DNA was cleaned from RNA by incubation with 10U of DNAse-free RNAseOne (Promega) at 37°C for 30 minutes. Following RNAseOne treatment the sample was supplemented with 4µl EDTA 0.5M and 8µl Tris-HCl pH 6.5 1M. Proteins were eliminated following a treatment with 1µg of ProteinaseK (SIGMA) at 45 °C for 1h. Finally the immunoprecipitated DNA was purified using the QIAquick PCR purification kit (QIAGEN) and was amplified using the Whole Genome Amplification kit (SIGMA).

ISWI ChIP-on-chip and data analysis

ChIP-on-chip experiments were performed using three biological

replicates. For each microarray hybridization experiment 1µg of immunoprecipitated or sonicated total input DNA was labeled with Cy3 and Cy5, respectively, and hybridized competitively on a NimbleGen *Drosophila* whole genome tiling 3-array set covering the entire fly genome (each array containing 385,000 spots of 50mer probes with a median probe spacing of 97bp). Genomic regions enriched in ISWI were identified using the Peak Score function that takes into account the length and intensity of the normalized raw $\log_2$(ChIPISWI/input) signals:

$$S = [\sum 1n \log_2(\text{ChIPISWI/input}) / n] + \sqrt{n}$$

S stands for Peak Score value, $\sum 1n \log_2$(ChIPISWI/input) is the sum of all $\log_2$(ChIPISWI/input) values of the probes under the peak, n is the number of probes under the peak and $\sqrt{n}$ is an empirically defined correction factor for the peak length contribution. Therefore, the Peak Score value is derived from two main variables: peak height, the mean $\log_2$(ratio) value of the probes below the peak; peak length, an empirical correction factor derived from the square root of the total number of probes belonging to a peak.

ISWI peaks were identified with the PeakPeaker tool, available in the CARPET program suite accessible through the Galaxy mirror site of IFOM- IEO- CAMPUS (http://host13.bioinfo3.ifom-ieo-campus.it:8080/) [82], using a -$\log_2$(p-values) threshold equal or greater than 9.5. The tool CARPET was also used to evaluate the relationship between the locations of ISWI peaks and the transcription start sites as well as to identify genes associated with ISWI peaks.

Detection of ChIP from Salivary Gland Chromatin

The immunoprecipitated DNA was analyzed by semiquantitative PCR using specific primers for representative ISWI enriched chromatin regions

(see genes in Figure 5 B-E) as well as sites of low ISWI association. For each pair of primers, the conditions of the PCR reaction were optimized to avoid saturation. Each experiment was analyzed at least twice. The following primers were used for the ISWI bound genes:

1. for *DLP-A*: F 5′-AATAGGCTCGCTGCATGAGT-3′, R 5′- CCTCTCACTCGCTCATTTCC-3′; *DLP-C*
F 5’-GGTGGAATTCACGTTACCTA-3’,
R- 5’- ACTCATGCCTCAGAATTGTC-3’;

2. for *CG10383-D*: F 5’-GAATGCTGGAGGTGGTGAAT-3’, R 5’- AACTAGCCGTTGGTGTGACC-3’, *CG10383-E*
F 5’-GGTCACACCAACGGCTAGT- 3’,
R 5’-ACGGGATTCACTCTGCAGTC -3’;

3. for *EcR-F*: F 5’-GGCGGTGATACGTGTATGTG-3’, R 5’- CTCCGAAGGACTGTTTTCCA -3’, *EcR-H*
F 5’- GACGCATATGGTGAGTGTGG -3’,
R 5’- GCGCCAAGACAAACACATTA-3’;

4. for *E2f-L*: F 5’- AAAAACGCTGTGTCAAGCTG-3’, R 5’- ATGCGATATGATGGCCTTTT-3’, *E2f-O*
F 5’-CAGTCCGCAAAAATGTGAAA-3’,
R 5’-GTGAGTACGTCGGTGGTGTG-3’,

5. for *CG8605 (*negative control corresponding to a gene with low ISWI chromatin association:*)*:
F 5’-GCTACAGGTGCATTCGAACA-3’,
R 5’- GCAAGAGATTTCTGCGTCGT-3’.

Osprey and Gorilla analysis

The Gene Ontology data were obtained from the Biogrid website (www.thebiogrid.org) and were represented in a graphical format using the Osprey software (http://biodata.mshri.on.ca/osprey/servlet/Index). For the GO analysis the gene annotation provided by FlyBase (www.flybase.org) were used with GOrilla (http://cbl-gorilla.cs.technion.ac.il/) to determine enriched GO terms.

MD Scan and MEME motif discovery analysis

The correlation existing between the number of occurrences of a motif M in a data set D of sequences obtained from the ISWI ChIP data, and the peak score corresponding to the same sequences was studied. In particular, were identified the most significant motifs with MDscan [69] or MEME [70], and were correlated the number of occurrences of the motifs within the sequence with the peak score of the sequence to which the motif belongs to. Spearman's correlation index was used as measure of the relationship between the number of occurrences of the motif within each sequence of the dataset and the peak score of the corresponding sequence according to the implementation of statistical computing environment R (http://www.r-project.org).

The Spearman rank assesses how well the relationship between two variables can be described using a monotonic function, that does not require specific assumptions about the distribution of the data. The sign of the Spearman correlation indicates the direction of association between two variables X and Y. If Y tends to increase when X increases, the Spearman correlation coefficient is positive. If Y tends to decrease when X increases, the Spearman correlation coefficient is negative. A Spearman

correlation of zero indicates that there is no tendency for Y to either increase or decrease when X increases. The Spearman correlation increases in magnitude as X and Y become closer to being perfect monotone functions of each other. When X and Y are perfectly monotonically related, the Spearman correlation coefficient becomes 1, otherwise is -1. Putative ISWI motif binding factors were identified querying the TRANSFAC and JASPAR databases to look for *D. melanogaster* homologues.

Nucleosomal DNA preparation

For each hybridization experiment ~150 wild-type and ~500 $ISWI^1$/$ISWI^2$ third-instar male or female larvae were dissected in DMM medium [81]. Batches of 10 larvae were processed as follows: salivary glands were transferred in eppendorf containing 100μl of M buffer (10mM HEPES, pH 7.6, 25mM KCl, 5mM MgCl2, 5% glycerol, 1mM PMSF, 1mM DTT) and were kept on ice. Nonidet-P40 was added to a final concentration of 0.5% and the mix was homogenized with 50 strokes using a plastic pestel on ice. Samples were centrifuged at 2,100g for 5 minutes at 4°C to pellet nuclei. The nuclear pellet was washed with 200μl of MNase buffer (10mM HEPES, pH 7.6, 25mM KCl, 5mM MgCl2, 5% glycerol, 2mM CaCl2, 1mM PMSF, 1mM DTT) and resuspended in 200μl of MNase buffer in the presence of 2 units of Microccocal nuclease (SIGMA) for 5 minutes at 26°C. The reaction was stopped with 200μl of S buffer (20mM Tris-HCl, pH 7.4, 200mM NaCl, 2mM EDTA, 2% SDS, 30mM EGTA) and treated with 200μg/ml of Proteinase K (SIGMA) for 1 hour at 37°C. Samples were extracted three times with phenol-chloroform, once with chloroform and were precipitated overnight with 1ml of absolute ethanol with 1μl Gene Elute-LPA (SIGMA) and 50μl of 3M

NaAcetate. Samples were centrifuged at 15,000g for 20 minutes at 4°C. The DNA pellet was washed with 70% ethanol and resuspended in 10μl of Nuclease free water and treated 15 minutes at 37°C with 5 units of DNase-free RNase ONE (Promega). Mononucleosomal DNA was purified by agarose gel isolation using Gel extraction kit (QIAGEN) and amplified with the Whole Genome Amplification kit (SIGMA). For each experiment 4μg of Cy3 labeled mononucleosomal DNA were used for the hybridization on the NimbleGen custom-tiled microarray.

Genomic DNA preparation

For each experiment about 50 male or female *wild-type* third-instar larvae and about 100 $ISWI^1$/$ISWI^2$ male or female larvae were collected, resuspended in 1ml of Larval Nuclear Buffer I [83] and homogenated with about 10 strokes in a Teflon Potter (Kontes Glass Co.) kept on ice. The homogenate was filtered through a layer of 64μm Nitex nylon meshwork (Genesee Scientific). Sample was centrifuged at 2,100g for 5minutes at 4°C. Surnatant was removed and the nuclear pellet washed three times with 500μl of M buffer. Pellet was resuspended in 400μl of MNase buffer and, after adding 400μl of S buffer, treated with 200μg/ml of proteinase K (SIGMA) for 1 hour at 37°C. Samples were three times phenol-chloroform extracted, once chloroform and overnight ethanol precipitated with 1μl Gene Eluite-LPA (SIGMA) and 0.3M NaAcetate. Samples were centrifuged at 15,000g for 20 minutes at 4°C. Pellet was washed with 70% ethanol and resuspended in 100μl of Nuclease free water and treated 15 minutes at 37°C with 20U DNase-free RNase ONE (Promega). Genomic DNA was sonicated for 4 minutes (60s on, 30s off) at the maximum power. Genomic DNA with a molecular weight between 100bp and 200bp was purified by gel isolation using Gel extraction kit (QIAGEN) and

amplified by WGA amplification kit (SIGMA). For each experiment 3μg of Cy5 labeled genomic DNA were used for NimbleGen custom-tiled microarray hybridization.

Nucleosome positioning array hybridization and data analysis

Salivary gland mononucleosomal DNA was purified and hybridized competitively against total larval GenDNA on a custom-tiled array .
Labelled genomic and mononucleosomal DNA were hybridized over a custom-tiled arrays containing 7.7Mbp of the *Drosophila* genome, in 385000 spots made of 50mer overlapped by 30bp. Microarray hybridizations were performed according to NimbleGen protocols. Microarray scanning and data extraction were conducted using NimbleScan software [84]. Nucleosome position data were derived from data coming from three biological replicates each for *wild-type* and for *ISWI* mutants.

Identification of nucleosome position differences between wild-type and ISWI mutants

In order to find regions containing changes in nucleosome positions between *wild-type* and *ISWI* mutant chromatin, was conducted an analysis using both the raw signal as well as the nucleosome classification of the MLM [74]. Differences in the raw signal were identified calculating the Z-score of the ratio between the *wild-type* and the *ISWI* mutant data tracks. Differences encompassing at least three probes with a Z-score value > / = 2 were extracted. These parameters are set to identify

differences equal to a shift of half a nucleosome.

Analysis of expected nucleosome occupancy near the TSS and at the 3' -end

To characterize the average nucleosome occupancy level at the TSS and 3'-end of the genes present in the nucleosome-tiled array, four lists of genes have been considered: all genes covered by the microarray, all genes repressed or overexpressed in ISWI mutant, all genes nearby the binding sites of ISWI. Fragments of length of 1000 bp centred at the TSS or at the 3'-end of each genes have been extracted from each one of the four lists. The average of nucleosomes occupancy of such extracted fragments was calculated and represented as a raw signal or MLM output.

ACKNOWLEDGMENTS

I would like to thank members of the laboratory, and Davide Corona for his precious feedbacks. I also would to thank Anna Sala for his contribution in the nucleosome positions analysis and Luca Pinello for his bioinformatic analysis.

This work was supported by grants from Fondazione Telethon, Giovanni Armenise Harvard Foundation, MIUR-FIRB, HFSP, AIRC and Compagnia San Paolo to D.F.V.C.

References

1. Xia, K., et al., *Impacts of protein-protein interaction domains on organism and network complexity.* Genome research, 2008. **18**(9): p. 1500-8.
2. Deuring, R., et al., *The ISWI chromatin-remodeling protein is required for gene expression and the maintenance of higher order chromatin structure in vivo.* Mol Cell, 2000. **5**(2): p. 355-65.
3. Stopka, T. and A.I. Skoultchi, *The ISWI ATPase Snf2h is required for early mouse development.* Proc Natl Acad Sci U S A, 2003. **100**(24): p. 14097-102.
4. Corona, D.F., et al., *ISWI is an ATP-dependent nucleosome remodeling factor.* Mol Cell, 1999. **3**(2): p. 239-45.
5. Deuring, R., et al., *The ISWI chromatin-remodeling protein is required for gene expression and the maintenance of higher order chromatin structure in vivo.* Molecular cell, 2000. **5**(2): p. 355-65.
6. Luger, K. and J.C. Hansen, *Nucleosome and chromatin fiber dynamics.* Current opinion in structural biology, 2005. **15**(2): p. 188-96.
7. Morales, V., et al., *Chromatin structure and dynamics: functional implications.* Biochimie, 2001. **83**(11-12): p. 1029-39.
8. Kingston, R.E. and G.J. Narlikar, *ATP-dependent remodeling and acetylation as regulators of chromatin fluidity.* Genes Dev, 1999. **13**(18): p. 2339-52.
9. Campos, E.I. and D. Reinberg, *Histones: annotating chromatin.* Annual review of genetics, 2009. **43**: p. 559-99.
10. Eberharter, A. and P.B. Becker, *ATP-dependent nucleosome remodelling: factors and functions.* J Cell Sci, 2004. **117**(Pt 17): p. 3707-11.

11. Hargreaves, D.C. and G.R. Crabtree, *ATP-dependent chromatin remodeling: genetics, genomics and mechanisms.* Cell research, 2011. **21**(3): p. 396-420.
12. Imhof, A., *Epigenetic regulators and histone modification.* Brief Funct Genomic Proteomic, 2006. **5**(3): p. 222-7.
13. Martin, C. and Y. Zhang, *Mechanisms of epigenetic inheritance.* Curr Opin Cell Biol, 2007. **19**(3): p. 266-72.
14. Horn, P.J. and C.L. Peterson, *Molecular biology. Chromatin higher order folding--wrapping up transcription.* Science, 2002. **297**(5588): p. 1824-7.
15. Kadonaga, J.T., *Eukaryotic transcription: an interlaced network of transcription factors and chromatin-modifying machines.* Cell, 1998. **92**(3): p. 307-13.
16. Li, B., M. Carey, and J.L. Workman, *The role of chromatin during transcription.* Cell, 2007. **128**(4): p. 707-19.
17. Shogren-Knaak, M., et al., *Histone H4-K16 acetylation controls chromatin structure and protein interactions.* Science, 2006. **311**(5762): p. 844-7.
18. Saha, A., J. Wittmeyer, and B.R. Cairns, *Chromatin remodelling: the industrial revolution of DNA around histones.* Nature reviews. Molecular cell biology, 2006. **7**(6): p. 437-47.
19. Imbalzano, A.N. and H. Xiao, *Functional properties of ATP-dependent chromatin remodeling enzymes.* Advances in protein chemistry, 2004. **67**: p. 157-79.
20. Peterson, C.L. and I. Herskowitz, *Characterization of the yeast SWI1, SWI2, and SWI3 genes, which encode a global activator of transcription.* Cell, 1992. **68**(3): p. 573-83.
21. Holstege, F.C., et al., *Dissecting the regulatory circuitry of a eukaryotic genome*. Cell, 1998. **95**(5): p. 717-28.

22. Sif, S., *ATP-dependent nucleosome remodeling complexes: enzymes tailored to deal with chromatin.* Journal of cellular biochemistry, 2004. **91**(6): p. 1087-98.
23. Trouche, D., et al., *RB and hbrm cooperate to repress the activation functions of E2F1.* Proceedings of the National Academy of Sciences of the United States of America, 1997. **94**(21): p. 11268-73.
24. Barrett, J.C., D.G. Thomassen, and T.W. Hesterberg, *Role of gene and chromosomal mutations in cell transformation.* Annals of the New York Academy of Sciences, 1983. **407**: p. 291-300.
25. Santos-Rosa, H. and C. Caldas, *Chromatin modifier enzymes, the histone code and cancer.* European journal of cancer, 2005. **41**(16): p. 2381-402.
26. Jones, P.A. and S.B. Baylin, *The epigenomics of cancer.* Cell, 2007. **128**(4): p. 683-92.
27. Sansam, C.G. and C.W. Roberts, *Epigenetics and cancer: altered chromatin remodeling via Snf5 loss leads to aberrant cell cycle regulation.* Cell cycle, 2006. **5**(6): p. 621-4.
28. Versteege, I., et al., *Truncating mutations of hSNF5/INI1 in aggressive paediatric cancer.* Nature, 1998. **394**(6689): p. 203-6.
29. Wilson, B.G. and C.W. Roberts, *SWI/SNF nucleosome remodellers and cancer.* Nature reviews. Cancer, 2011. **11**(7): p. 481-92.
30. Lee, D., et al., *SWI/SNF complex interacts with tumor suppressor p53 and is necessary for the activation of p53-mediated transcription.* The Journal of biological chemistry, 2002. **277**(25): p. 22330-7.
31. Andersen, E.C., X. Lu, and H.R. Horvitz, *C. elegans ISWI and NURF301 antagonize an Rb-like pathway in the determination of multiple cell fates.* Development, 2006. **133**(14): p. 2695-704.

32. Mohamed, M.A., et al., *Epigenetic events, remodelling enzymes and their relationship to chromatin organization in prostatic intraepithelial neoplasia and prostatic adenocarcinoma*. BJU international, 2007. **99**(4): p. 908-15.
33. Stopka, T. and A.I. Skoultchi, *The ISWI ATPase Snf2h is required for early mouse development.* Proceedings of the National Academy of Sciences of the United States of America, 2003. **100**(24): p. 14097-102.
34. Jin, J., et al., *A mammalian chromatin remodeling complex with similarities to the yeast INO80 complex.* The Journal of biological chemistry, 2005. **280**(50): p. 41207-12.
35. van Attikum, H. and S.M. Gasser, *ATP-dependent chromatin remodeling and DNA double-strand break repair.* Cell cycle, 2005. **4**(8): p. 1011-4.
36. Morrison, A.J., et al., *INO80 and gamma-H2AX interaction links ATP-dependent chromatin remodeling to DNA damage repair.* Cell, 2004. **119**(6): p. 767-75.
37. Corona, D.F. and J.W. Tamkun, *Multiple roles for ISWI in transcription, chromosome organization and DNA replication.* Biochim Biophys Acta, 2004. **1677**(1-3): p. 113-9.
38. Lusser, A. and J.T. Kadonaga, *Chromatin remodeling by ATP-dependent molecular machines.* BioEssays : news and reviews in molecular, cellular and developmental biology, 2003. **25**(12): p. 1192-200.
39. Bao, Y. and X. Shen, *SnapShot: chromatin remodeling complexes.* Cell, 2007. **129**(3): p. 632.
40. Dirscherl, S.S. and J.E. Krebs, *Functional diversity of ISWI complexes.* Biochemistry and cell biology = Biochimie et biologie cellulaire, 2004. **82**(4): p. 482-9.

41. Elfring, L.K., et al., *Genetic analysis of brahma: the Drosophila homolog of the yeast chromatin remodeling factor SWI2/SNF2.* Genetics, 1998. **148**(1): p. 251-65.
42. Tsukiyama, T., et al., *ISWI, a member of the SWI2/SNF2 ATPase family, encodes the 140 kDa subunit of the nucleosome remodeling factor*. Cell, 1995. **83**(6): p. 1021-6.
43. Tsukiyama, T. and C. Wu, *Purification and properties of an ATP-dependent nucleosome remodeling factor*. Cell, 1995. **83**(6): p. 1011-20.
44. Varga-Weisz, P.D., et al., *Chromatin-remodelling factor CHRAC contains the ATPases ISWI and topoisomerase II.* Nature, 1997. **388**(6642): p. 598-602.
45. Ito, T., et al., *ACF, an ISWI-containing and ATP-utilizing chromatin assembly and remodeling factor.* Cell, 1997. **90**(1): p. 145-55.
46. Eisen, J.A., K.S. Sweder, and P.C. Hanawalt, *Evolution of the SNF2 family of proteins: subfamilies with distinct sequences and functions.* Nucleic acids research, 1995. **23**(14): p. 2715-23.
47. Bork, P. and E.V. Koonin, *An expanding family of helicases within the 'DEAD/H' superfamily.* Nucleic Acids Res, 1993. **21**(3): p. 751-2.
48. Boyer, L.A., R.R. Latek, and C.L. Peterson, *The SANT domain: a unique histone-tail-binding module?* Nature reviews. Molecular cell biology, 2004. **5**(2): p. 158-63.
49. Grune, T., et al., *Crystal structure and functional analysis of a nucleosome recognition module of the remodeling factor ISWI.* Molecular cell, 2003. **12**(2): p. 449-60.

50. Hota, S.K. and B. Bartholomew, *Diversity of operation in ATP-dependent chromatin remodelers.* Biochimica et biophysica acta, 2011. **1809**(9): p. 476-87.
51. Eberharter, A. and P.B. Becker, *ATP-dependent nucleosome remodelling: factors and functions.* Journal of cell science, 2004. **117**(Pt 17): p. 3707-11.
52. Langst, G. and P.B. Becker, *Nucleosome mobilization and positioning by ISWI-containing chromatin-remodeling factors.* Journal of cell science, 2001. **114**(Pt 14): p. 2561-8.
53. Clapier, C.R. and B.R. Cairns, *The biology of chromatin remodeling complexes.* Annual review of biochemistry, 2009. **78**: p. 273-304.
54. Narlikar, G.J., H.Y. Fan, and R.E. Kingston, *Cooperation between complexes that regulate chromatin structure and transcription.* Cell, 2002. **108**(4): p. 475-87.
55. Tsukiyama, T., P.B. Becker, and C. Wu, *ATP-dependent nucleosome disruption at a heat-shock promoter mediated by binding of GAGA transcription factor.* Nature, 1994. **367**(6463): p. 525-32.
56. Mizuguchi, G., et al., *Role of nucleosome remodeling factor NURF in transcriptional activation of chromatin.* Molecular cell, 1997. **1**(1): p. 141-50.
57. Precht, P., A.L. Wurster, and M.J. Pazin, *The SNF2H chromatin remodeling enzyme has opposing effects on cytokine gene expression.* Molecular immunology, 2010. **47**(11-12): p. 2038-46.
58. Goldmark, J.P., et al., *The Isw2 chromatin remodeling complex represses early meiotic genes upon recruitment by Ume6p.* Cell, 2000. **103**(3): p. 423-33.

59. Strohner, R., et al., *NoRC--a novel member of mammalian ISWI-containing chromatin remodeling machines.* The EMBO journal, 2001. **20**(17): p. 4892-900.
60. Collins, N., et al., *An ACF1-ISWI chromatin-remodeling complex is required for DNA replication through heterochromatin.* Nature genetics, 2002. **32**(4): p. 627-32.
61. Vincent, J.A., T.J. Kwong, and T. Tsukiyama, *ATP-dependent chromatin remodeling shapes the DNA replication landscape.* Nature structural & molecular biology, 2008. **15**(5): p. 477-84.
62. Badenhorst, P., et al., *Biological functions of the ISWI chromatin remodeling complex NURF.* Genes & development, 2002. **16**(24): p. 3186-98.
63. Perpelescu, M., et al., *Active establishment of centromeric CENP-A chromatin by RSF complex.* The Journal of cell biology, 2009. **185**(3): p. 397-407.
64. Yokoyama, H., et al., *ISWI is a RanGTP-dependent MAP required for chromosome segregation.* The Journal of cell biology, 2009. **187**(6): p. 813-29.
65. Agabiti, N., et al., *The association of socioeconomic disadvantage with postoperative complications after major elective cardiovascular surgery.* Journal of epidemiology and community health, 2008. **62**(10): p. 882-9.
66. Corona, D.F., et al., *ISWI regulates higher-order chromatin structure and histone H1 assembly in vivo.* PLoS Biol, 2007. **5**(9): p. e232.
67. Deng, D., Z. Liu, and Y. Du, *Epigenetic alterations as cancer diagnostic, prognostic, and predictive biomarkers.* Adv Genet, 2010. **71**: p. 125-76.

68. Dirscherl, S.S. and J.E. Krebs, *Functional diversity of ISWI complexes.* Biochem Cell Biol, 2004. **82**(4): p. 482-9.
69. Liu, X.S., D.L. Brutlag, and J.S. Liu, *An algorithm for finding protein-DNA binding sites with applications to chromatin-immunoprecipitation microarray experiments.* Nat Biotechnol, 2002. **20**(8): p. 835-9.
70. Bailey, T.L., et al., *MEME: discovering and analyzing DNA and protein sequence motifs.* Nucleic Acids Res, 2006. **34**(Web Server issue): p. W369-73.
71. Johansen, K.M., et al., *Chromatin structure and nuclear remodeling.* Crit Rev Eukaryot Gene Expr, 1999. **9**(3-4): p. 267-77.
72. Stephens, G.E., et al., *Immunofluorescent staining of polytene chromosomes: exploiting genetic tools.* Methods Enzymol, 2004. **376**: p. 372-93.
73. Yuan, G.C., et al., *Genome-scale identification of nucleosome positions in S. cerevisiae.* Science, 2005. **309**(5734): p. 626-30.
74. Di Gesu, V., et al., *A multi-layer method to study genome-scale positions of nucleosomes.* Genomics, 2009. **93**(2): p. 140-5.
75. Park, Y. and M.I. Kuroda, *Epigenetic aspects of X-chromosome dosage compensation.* Science, 2001. **293**(5532): p. 1083-5.
76. Smith, E.R., C.D. Allis, and J.C. Lucchesi, *Linking global histone acetylation to the transcription enhancement of X-chromosomal genes in Drosophila males.* J Biol Chem, 2001. **276**(34): p. 31483-6.
77. Larschan, E., et al., *MSL complex is attracted to genes marked by H3K36 trimethylation using a sequence-independent mechanism.* Mol Cell, 2007. **28**(1): p. 121-33.
78. Holstege, F.C., et al., *Dissecting the regulatory circuitry of a eukaryotic genome.* Cell, 1998. **95**(5): p. 717-28.

79. Corona, D.F., et al., *Modulation of ISWI function by site-specific histone acetylation.* EMBO reports, 2002. **3**(3): p. 242-7.
80. Burgio, G., et al., *Genetic identification of a network of factors that functionally interact with the nucleosome remodeling ATPase ISWI.* PLoS Genet, 2008. **4**(6): p. e1000089.
81. Collesano, M. and D.F. Corona, *Flow cytometry and karyotype analysis of D.melanogaster eye disc cells.* Fly, 2007. **1**(4): p. 242-4.
82. Cesaroni, M., et al., *CARPET: a web-based package for the analysis of ChIP-chip and expression tiling data.* Bioinformatics, 2008. **24**(24): p. 2918-20.
83. La Rocca, G., G. Burgio, and D.F. Corona, *A protein nuclear extract from D. melanogaster larval tissues.* Fly, 2007. **1**(6): p. 343-5.
84. Kim, T.H., et al., *A high-resolution map of active promoters in the human genome.* Nature, 2005. **436**(7052): p. 876-80.